THE IDENTIFICATION AND QUANTIFICATION OF FULL-DEPTH PATCHING NEED USING REMOTE SENSING TECHNOLOGY

A Dissertation
Presented to
The Academic Faculty

by

Geoffrey L. Price

In Partial Fulfillment
of the Requirements for the Degree
Master of Science in the
School of Civil and Environmental Engineering

Georgia Institute of Technology
AUGUST 2017

THE IDENTIFICATION AND QUANTIFICATION OF FULL-DEPTH PATCHING NEED USING REMOTE SENSING TECHNOLOGY

Approved by:

Dr. Yi-Chang Tsai, Advisor
School of Civil and Environmental Engineering
Georgia Institute of Technology

Dr. James Lai
School of Civil and Environmental Engineering
Georgia Institute of Technology

Dr. Zhaohua Wang
Center for Geographic Information Systems
Georgia Institute of Technology

Date Approved: July 27, 2017

To my mother, my father, and my sister

ACKNOWLEDGEMENTS

I would like to begin by thanking Dr. Tsai for his work and encouragement beginning in my time as an undergraduate student and continuing through graduate school. His instruction has taught me to use critical thinking to efficiently deconstruct complex problems into simpler pieces, all while not letting go of the overarching narrative and purpose. Because of his guidance and kindness, I am a more confident person and a more effective communicator. I would also like to thank Dr. Chengbo Ai, Dr. Zhaohua Wang, and Yi-Ching Wu for their tremendous support over the years. Their guidance in research, and life, has helped me develop a strong base on which to build my career.

I would also like to thank the group of graduate students working in Dr. Tsai's research group including Anirban, April, Cibi, Georgene, Lauren, Ross, Segolene, Vincent, and Yifei. I have enjoyed collaborating with them over the years and I wish them all much success in their academic and professional careers. I would also like to thank Ali Etezady and Daejin Kim, and Himanshu Wad for their companionship and support throughout our years at Georgia Tech.

Lastly, I would like to thank my family. I would like to thank my mother, father, and sister for their unceasing support and praise. I would not have been able to accomplish half of my achievements without their love and support.

TABLE OF CONTENTS

LIST OF TABLES

LIST OF FIGURES

LIST OF SYMBOLS AND ABBREVIATIONS

AADT	Annual Average Daily Traffic
ANN/NN	Artificial Neural Network / Neural Network
ASCE	American Society of Civil Engineers
B	Broken
C	Crumbling
CFE	Crack Fundamental Element
CTI	Crack Type Index
DOT	Department of Transportation
DP	Deep Patching image
GDOT	Georgia Department of Transportation
GPR	Ground-Penetrating Radar
GPS	Global Positioning System
HNN	Histogram-based Neural Network
I	Intact
INN	Image-based Neural Network
LCMS	Laser Crack Measurement System
LWW	Length-Weighted Width
MCD	Maximum Inter-Centroid Distance
MCW	Maximum Crack Width
MNC	Minimum Number of Centroids
NCDOT	North Carolina Department of Transportation

NDP	No Deep Patching image
PACES	Pavement Condition Evaluation System
PMS	Pavement Maintenance System/Schedule
PNN	Proximity-based Neural Network
RCW	Representative Crack Width
TCL	Total Crack Length
US80	US Highway 80 near Savannah, GA
XML	Extensible Markup Language

SUMMARY

Start In this thesis, a methodology is proposed for identifying pavement patching locations based on the pavement cracking characteristics observed from the surface. The objective of the research was to adapt and improve upon current crack classification methods for use in identifying full-depth patching locations which are characterized by severe alligator cracking. Using input from an experienced pavement engineer, the characteristics of full-depth patching locations are assessed including the total crack length in an area, the crack density, the average crack width, and the spatial distribution of polygons formed by cracks. Using these characteristics, crack detection results are processed to determine the need for full-depth patching.

The second chapter outlines the methodology for identifying the full-depth patching locations. To limit the amount of processing needed, the original crack detection results for the 5-by-2.08 m. pavement images are classified as deep patching image (DP) candidates or no deep patching images (NDP) based on the total crack length, average crack width, and the density of cracking. It is determined that a total crack length of 12.2-m, an average crack width of 14.0-mm, and a crack node density of 70 nodes / 250-mm are sufficient criteria for identifying over 95% of pavement images requiring full-depth patching. Images that meet these criteria are classified as DP images; otherwise the image is classified as NDP. Once this high-level classification process is complete, the crack detection results are used to identify the need for patching in the images.

The candidate DP images are processed to create binary crack maps which are then processed to identify the polygons which are the basis for alligator cracking. Once the polygons are identified, they are clustered to determine if there is a need for patching within the image. Using a spatial clustering algorithm, the centroids of the crack polygons are clustered together if they are within 711-mm (2.33-ft) of each other. Clusters of three or fewer centroids are rejected, and all other clusters are considered as candidate patching locations. These candidate patches are then further reduced by removing any patches shorter than 2-ft in length in the driving direction. After removing these patches that are too short, all remaining patches are identified by their length and location. In addition to identifying the patching areas, a study is performed to determine if surface cracking characteristics correlate with the depth of pavement distresses.

Full-depth patching requires removing all defective pavements and therefore requires estimating the depth of pavement distress. To better understand subsurface conditions, pavement cores are taken from pavements in various stages of distress on US80 in 2016. The pavement core characteristics including crack depth, crack width, and the density of cracking in a window surrounding the core, are measured for 13 cracked pavement cores and these data are used to assess the correlation between pavement surface condition and the depth of distress. It is concluded that cores taken from less deteriorated pavements will have cracks less than 3-in. deep and cores located near alligator cracking typically have cracking deeper than 6-in. However, it is difficult to measure the full depth of distress for cores located near alligator cracking because the crumbling pavement causes the core to fall apart. Because of this, it is difficult to accurately predict the distress depth

using only surface characteristics, but in the cases observed, the cracking consistently occurred more than 6-in. below the surface.

Using pavement cracking data from 2011, 2013, and 2015, the need for full-depth patching on US80/SR26 EB MP 10 – 11 is analyzed to track the growth and identify locations that have accelerated damage to the pavement. The one mile of data is separated into 4 x 100-ft + 24 x 200-ft + 1 x 80-ft = 29 sections. Most growth occurs between stations MP 10 + 3000 and MP10 + 4000. The two 200-ft sections beginning at MP10 + 3000 and MP10 + 3400' are analyzed because of their extreme deterioration over the four-year period. It is determined that roadway geometry appears to significantly affect the deterioration rate. The counter-clockwise horizontal curve leads to significant damage in the right lane side as vehicles and heavy trucks apply more weight to the right wheel path than the left. The analysis shows the strength of the proposed method at identifying full-depth patching areas as well as for tracking growth over time.

The proposed method builds upon previous pavement crack classification methods to identify pavement locations that are likely to have severe damage to the base layers. The method shows promise for future use in the field by pavement experts to identify patching need and estimate the quantity of material being removed. This information can be used to help make more informed decisions when allocating and prioritizing funding for roadway reconstruction projects. Additionally, the proposed method is easily adaptable, allowing for separate agencies to use it with ease.

CHAPTER 1. INTRODUCTION

In their 2017 report card on infrastructure in the United States, the American Society of Civil Engineers (ASCE) assigned a 'D' grade for the condition of the nation's roads, stating that approximately "one out of every five miles of highway pavement is in poor condition" and that there is an estimated $420 billion backlog for repairing existing highways [1]. The decline in national pavement condition and increase in repair backlog are the result of a lack of funding in recent years combined with an increase in vehicular miles traveled (VMT). The increase in VMT results in more damage to the pavement structure. As the condition of the nation's roads continues to decline due to insufficient funding, more expensive and labor-intensive maintenance is required to bring the system to a satisfactory condition.

Flexible pavements, which make up most of the pavement infrastructure, are kept in good condition by performing periodic maintenance designed to maintain a state of good repair. These plans, known as pavement management systems (PMS), are designed to maintain a smooth surface and remove existing distresses such as cracking, rutting, raveling, and others. In recent years, inadequate funding has caused delays in maintenance, severely impacting maintenance schedules while allowing pavement condition to deteriorate to the point of losing severe structural quality, known as failure [2]. As the pavement deteriorates, cracks form in the top and bottom of the asphalt layers. As these cracks grow, widen, and deepen, traditional fixes such as resurfacing and crack sealing become less effective treatments. Additionally, if left untreated, water and other foreign materials enter the pavement structure through the surface cracks, accelerating the

deterioration of the pavement as the asphalt material is washed away and the structure loses its load-carrying capacity. This accelerated deterioration can lead to severe cracking in multiple pavement layers resulting in poor ride quality, severe rutting in the wheel paths, and eventually potholes.

To improve the ride quality and restore the pavement condition, the failed surface and base layers must be removed until a smooth, structurally sound layer is found. Once the failed pavement is removed, the resulting hole is filled with asphalt material, typically Hot-mix asphalt (HMA), and compacted. This process is typically known as full-depth patching, but may also be referred to as ‘deep patching’ or ‘spot reconstruction.’ Through this process, the pavement surface is restored and the failed material is replaced, significantly extending the life of the pavement. However, because of the labor, materials and time needed, this procedure is costly and is typically only performed when the ride quality is severely reduced and/or there is significant damage to the surface and base layers.

To ensure this procedure is only performed where needed, full-depth patching locations are identified in the field by pavement experts trained to use surface characteristics to identify locations with poor base quality and in need of repair. These locations are identified through an inspection performed by engineers where the pavement is visually reviewed either from a vehicle or the side of the road. Through this inspection, the locations requiring full-depth patching are identified and marked by surveyors. After identification, the amount of patching needed is quantified as a volume measurement. This volume represents the total material needed to backfill the patched locations after removing the defective pavement.

1.1 Current Practice for Full-Depth Patching Identification

Currently, most patch identification and quantification is done manually by engineers in the field. Typically, after the initiation of a pavement rehabilitation or reconstruction project, engineers perform inspections to identify locations in need of full-depth patching. These inspections are performed by the roadside which may expose inspectors to moving traffic. In addition to being a safety hazard, these roadside inspections are time-consuming and labor intensive, requiring engineers to manually mark with paint all locations in need of full-depth patching. These areas are identified in advance so they can be prioritized for maintenance.

Full-depth patching is often prioritized over other maintenance practices because of the associated costs and labor; however, limited funds often mean that less distressed patching locations are ignored and allowed to deteriorate and only the most severe of patches are fixed. This increases future costs because the smaller patching areas quickly deteriorate and grow. Locations with base problem need proper maintenance to avoid additional funding and maintenance work in the future after the locations have deteriorated. To facilitate proper identification, surveys are performed by expert engineers who are trained to understand the characteristics of pavements that have failed and require reconstruction of their base layers.

In the field, the engineers identifying full-depth patching locations are trained to identify the characteristics of pavement that is failing or has begun to fail. One of the primary distresses indicative of pavement condition is load/fatigue cracking. This type of cracking results from repeated traffic loads being applied to the pavement surface,

eventually causing cracks to form in the pavement wheel paths [3]. This type of cracking begins as a single longitudinal crack and, over time, appears as a series of interconnected cracks that resemble an alligator hide. This type of distress is illustrated in Figure 1-1.

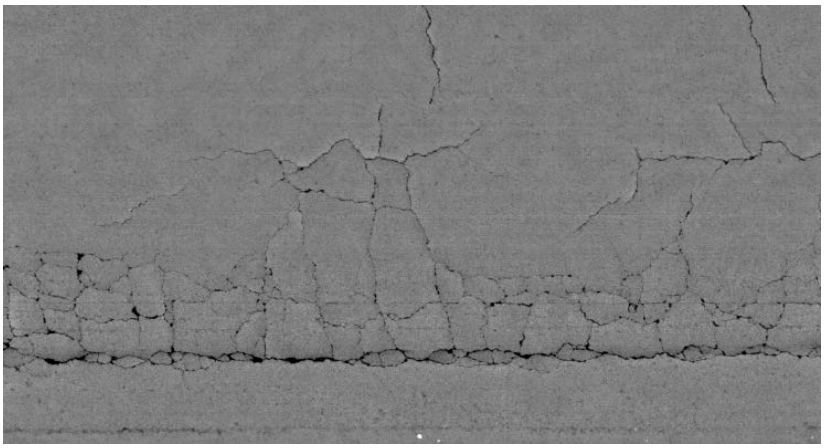

Figure 1-1 Alligator cracking covering the wheel path and pavement edge

For this reason, this type of cracking is referred to as alligator cracking by many DOTs and transportation agencies. Repeated cyclic loading causes severe breakage in multiple pavement layers leading to this appearance.

This type of cracking results in a reduction in riding comfort and eventually leads to potholes as the polygons formed by cracks pop out from the surface. Additionally, the cracks allow in water/foreign materials, eroding the base layers under the cracks and causing significant rutting (>1/4”) in the wheel paths. Typically, these indicators are what surveyors use in the field to identify patching locations. Identifying severe alligator cracking is critical because not identifying locations with this distress can have adverse consequences as shown in Figure 1-2.

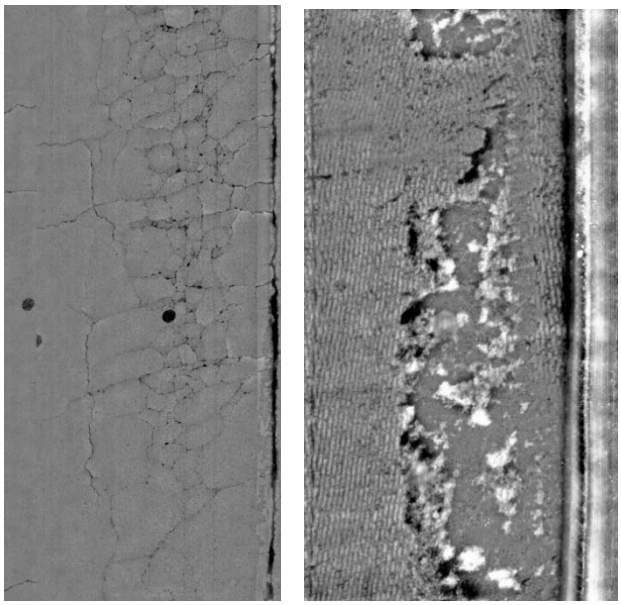

(a) (b)

Figure 1-2 Distressed pavement (a) before and (b) after 1-in. milling

This figure illustrates the consequences of not properly identifying full-depth patching areas. In Figure 1-2a, the road surface prior to traditional 1-inch milling is shown. The same location is shown in Figure 1-2b after the top 1-inch of pavement was removed. The milled surface clearly shows distress, cracking, and crumbling of the pavement which would not provide a strong base on which to lay new pavement. These locations are important to identify during a pavement inspection because a crumbling base will soon lead to a cracked and distressed surface. Cracking is the main indicator of the need for full-depth patching; however, there are some other distresses such as potholes and previous semi-permanent patches that are patched because they are indicative of base layer failure. Once identified, these distressed locations are quantified so the total cost and need for materials can be estimated.

Typically, the volume of patching material needed for full-depth patching operations is estimated either using a constant depth or a varying depth. For some transportation agencies, regardless of the severity of cracking for the patch, a constant depth is used with the distressed area of the patch to estimate the volume of material to be removed. For example, in the Iowa DOT, full-depth patches are dug to the thickness of the HMA pavement, but no less than 9 in. and no more than 15 in [4]. In contrast, other agencies may attempt to estimate the depth of material to be removed based on the severity of cracking visually observed on the surface during the manual inspection. Both of these approaches may not be sufficient at adequately assessing the depth of material to be removed and, therefore, may result in overestimation or underestimation of costs, labor, and materials.

Although these pavement condition inspections are typically performed manually, certain efforts have been made in recent years to reduce the costly and labor-intensive work required in performing these surveys by employing emerging remote sensing technologies capable of collecting high-resolution pavement surface data automatically [5]. Remote sensing is the application of sensing technologies to observe object characteristics from a distance. Through this procedure pavement surface can be scanned using high-resolution lasers and the collected laser information can be processed to identify the same pavement distresses engineers identify in the field while also improving the safety and speed of the survey.

1.2 Using Advanced Technology to Identify and Quantify Full-Depth Patching Need

Although no literature was found pertaining to using remote technology to assess the need for maintenance activities such as full-depth patching, significant research has been made into identifying and classifying alligator cracking from other types of cracking that do not indicate a need for full-depth patching. The following sections describe the various methods that have been used to identify and characterize alligator cracking using advanced technology.

1.2.1 Identifying Full-Depth Patching Need Using Crack Classification

There has been an increase in recent years of using advanced technology, including high-speed cameras, line-laser profilers, and GPS (global positioning systems), and others, in transportation asset management procedures. In a 2013 NCDOT report, 50 state DOTs were surveyed on their methods for collection of data for transportation assets and pavement condition. Of the 35 respondent states, 18 reported using automated methods to collect data for pavement and/or other roadway assets, and of these, 11 specifically collect pavement data [6]. Remote collection of pavement is beneficial because the images can be processed internally to assess the pavement condition, significantly reducing the amount of time spent in the field performing inspections.

To assess pavement condition, the pavement distresses need to be identified, classified, and quantified. In recent years, there has been much interest in identifying pavement distresses using both 2D and 3D images of the surface. Once the distresses are detected, the next step is to classify the distresses by severity. Classifying pavement

cracking has been explored thoroughly using various methods which typically fall into one or more of three categories: 1) projection, 2) feature extraction, and 3) artificial intelligence, which are explained in the following sections. These methods are not mutually exclusive, and can be combined for classification that is more accurate. The following sections outline the three categories of classification and give examples of research that has been done involving each method.

1.2.2 Projection and Hough Transform for Crack Classification

When using projection for crack classification, a binary image is created through image processing from the 2D or 3D surface image. In this binary image, the crack pixels are represented with a value of '1' (typically shown in white) and any background pixels (black) that are not of interest are given a value of '0.' Projection involves projecting the crack pixels to a horizontal, vertical, or diagonal axis resulting in a histogram of pixel density. This histogram can be used to assess the distribution of pixels along the projected plane and the difference between adjacent histogram values (known as 'proximity') can be used to assess crack density and classify cracking images. Alternatively, the number of cracks in an image can be determined using a Hough transform, which projects the pixels from a detected crack onto a series of axes at different angles to determine the number of cracks and their orientation.

Mohajeri and Manning process pavement images from a video log into binary images. The crack pixels are then projected to the X and Y axes and the rows and columns with > 50% crack pixels are compared to threshold values to classify as one of seven types of cracking. The method proves suitable for analysis of crack type and

severity when compared to crack statistics measured in-field. [7]. Similarly, Rababaah et al segment images and use a Hough transform to get average crack angle and number of cracks. Direct projection to the X and Y axes is also used to create normalized histograms known as feature vectors. These vectors are used to estimate crack type (longitudinal, alligator, block, or transverse). Results show that using projection to create a feature vector was more effective as an input than the result from the Hough transform. Results show 100% classification of alligator cracks from longitudinal, transverse, and block cracking images; however, the size of the alligator cracking data set is not given [8].

Chua and Xu collect 480 x 480-pixel pavement images and sum gray levels in the longitudinal (driving) and transverse directions. The two resultant arrays are then used to identify distress zones in the image, which are typically the pavement cracks. The type of cracking (transverse, longitudinal, diagonal, alligator, map cracking, and no distress) is estimated using the dimensions of the distress zone, the pixel intensity values, and the estimated width of the crack distress. This method achieves 80% accuracy when identifying alligator cracks; however the images used are susceptible to misclassification due to changes in lighting and shadows in the captured images [9].

Lee and Kim use the projected histogram data in binary crack images to develop a crack type index (CTI). The sums of differences in adjacent histogram values for the horizontal and vertical directions are calculated. Using these values, CTI is calculated as the sum of vertical differences minus the sum of horizontal differences. In this way, large positive numbers indicate longitudinal cracking, values near zero indicate alligator cracking or block cracking, and negative values indicate transverse cracks. This method

achieves 90.7% accuracy overall with 85% accuracy for classifying alligator cracking images [10].

Projection and Hough transformation has also been used by Cheng et al as a method of testing crack detection results. Cheng uses projection of crack pixels in four different directions to classify binary cracking images. The crack pixels are projected onto horizontal planes at 0°, 45°, 90°, and 135°. The peak values from these projections are then compared to a threshold value. The projection results show alligator cracking can be easily identified from the peak values of the histogram projections; however, in this experiment, the sample size of alligator cracking images was limited. The strong results from these studies indicate projection is efficient at identifying and classifying pavement cracks [11].

Projection of crack pixels to different axes is useful for identifying crack directionality as well as measuring crack density which is an important feature of identifying alligator cracking. However, crack projection often relies on image segmentation which can be disadvantageous for identifying alligator cracking if an appropriate window size is not chosen. By splitting the original pavement images into sub-images, the full topology is not considered when assigning a classification. Additionally, projection requires use of a 2D pavement image which does not take account for the shape of the surface. When identifying full-depth patching locations, the shape of the pavement surface and the surrounding pavement topology are important in determining if patching is required.

To incorporate more advanced analysis of pavement images, a more complex classification method is required to process the large amount of image data. Many researchers have used attempted to train artificial intelligence programs known as neural networks to identify and classify pavement images. Neural networks are beneficial because they can be trained to large images as input and can therefore assess the entirety of the pavement topology rather than sub-images. The next section discusses the use of neural networks as trainable classifiers for pavement crack classification.

1.2.3 Artificial Intelligence-based Crack Classification

Because asphalt cracking becomes more complex as the pavement deteriorates, significant research has been done to artificially capture the growth of complexity using artificial intelligence, particularly through artificial neural networks (ANN). These ANN, sometimes abbreviated neural networks (NN), can be modified in terms of size and complexity to allow for different types and sizes of input. This ability to change in size and shape makes this method feasible for classifying images regardless of size.

Using a combination of classification methods, Saar and Talvik use the X and Y histogram vectors from projection, as well as the medians and max values of these vectors, as input to a neural network. The classifier achieves >95% accuracy for longitudinal and transverse cracks, but accuracy for alligator cracking is 84% [12]. The poor alligator cracking classification performance is, in part, due to the inability of the NN to differentiate block cracking from alligator cracking. Because the two classifications have similar distributions of horizontal and vertical cracks, it is difficult

for classifiers to distinguish. To help with this issue, many researchers use projection and feature extraction results as additional input to NN classifiers.

Lee and Lee use an image-based neural network (INN), a histogram-based neural network (HNN), and a proximity-based neural network (PNN) as classifiers. Using different training and testing methods, the INN, HNN, and PNN classifiers achieve an accuracy of 70.2%, 75% and 95.2% respectively. Of the three classifiers, the HNN and PNN struggle with differentiating block and alligator cracking [13]. In addition to issues with classifying alligator cracking, using NN classifiers requires significant time for training and testing the classifier to determine the optimal classifier settings. For NN classifiers to perform well, the input and the NN structure must be carefully constructed.

Chou et al use weighted averages of pixel intensities, called moment invariants, of different images with predetermined classifications to train a neural network to classify images based on seven different classifications. Image moments can be used to estimate properties of binary images including crack area, the centroid of cracking, and the crack orientation. Chou et al. use moment functions developed by Hu, Bamieh, and Zernike to assess shape, directionality, and density of shapes in grayscale pavement images. Results show 100% classification of the 115 test images into the seven classifications [14]. Moment invariants are feasible for use in a NN classifier, but the classifier still required significant training to achieve the given results.

Kaseko et al compare the merits of the Bayes and *k*-nearest neighbor (k-NN) classifiers against the multilayer feed-forward (MLF) neural network and two-stage piecewise linear neural network classifiers. The traditional Bayes and k-nearest neighbor

classifiers assume a statistical model of the data and use appropriate parameters to classify. The MLF and two-stage piecewise classifiers use different structures of neural networks to determine output given sufficient training. Results show high total accuracy (>90%) for all classifiers except the Bayes classifier. The neural classifiers performed well with 93.0 and 93.9% accuracy for the MLF and piecewise linear classifiers respectively. However, these neural classifiers required extensive training and modification of parameters such as to achieve the posted results [15].

Neural networks are a powerful tool for accurate classification, but they typically require extensive training and testing to achieve high accuracy. Additionally, once trained, they are not easily adapted for other purposes. For full-depth patching location identification, classification algorithms may need to be adapted to accommodate the pavement rehabilitation strategies of different transportation agencies. Additionally, these agencies may be interested in understanding the process behind classification, which is not possible with neural networks. Neural networks are akin to black boxes, and therefore cannot relay information that is used to better understand the classification results. For more in-depth knowledge of how classification decisions are made, many researchers have used image processing to identify and extract features from pavement images.

1.2.4 Feature Extraction for Crack Classification

Feature extraction is the identification of specific cracking characteristics that can be used to classify cracking images. Crack features may include crack dimensions such as length, width, and depth, as well as crack topology such as crack branch points, end points, and polygons. As pavement deteriorates, these features may change in number,

size, shape, and dimension. Feature extraction is used to create, for the different features, threshold values that define the different classifications of cracking.

Koutsopoulos et al improve upon previous classification methods proposed by Koutsopoulos and El Sanhouri [16] which performed poorly when classifying alligator cracking and block cracking. After performing image processing to identify distresses, images are divided into subsections and each is assigned one of six symbols (primitives) based on the orientation and organization of distress pixels. The distress type is then determined, per two different models, based on the presence of different primitives in the image. Results show 83% classification on the small test data set of six alligator cracking images [17]. To better understand the advantage of using features, a larger data set is required.

Georgopoulos et al divide pavement images into crack tiles and classify the tiles as ‘distressed’ or ‘no distresses based on the number of crack pixels in the tile. The distressed areas are connected to form vectors according to the orientation of cracking in the tiles, and based on the presence of horizontal and vertical vectors in the collective crack tiles, the original images are classified as having transverse, longitudinal, or alligator/block cracking. ‘Alligator/block’ images are further classified based on the size of the polygons in the image. Results show 100% classification of alligator cracking; however, the severity of the alligator cracking images was only classified correctly for 50% of the images [18].

In a recent study conducted by Tsai et al [19] use a multi-scale crack fundamental element (CFE) model developed by Yuchun and Tsai to group pavement cracks at

different scales. Through this method, small crack pieces are aggregated to crack curves and networks before combining to form a single CFE. As the scale of the CFE increases, more crack characteristics are added, allowing for a full analysis of the image cracking at different levels. This method shows potential for adaptation to different transportation agencies' performance metrics by providing information from the large-scale crack groups to the small-scale crack segments. Results show this model is easily adaptable to GDOT's Pavement Condition Evaluation System (PACES) and achieves 95% accuracy of the two severities of fatigue cracking identified as alligator cracking [20, 21].

Of the multiple approaches to classifying pavement cracking, feature extraction best attempts to model the logic of pavement experts in field by identifying characteristics intrinsic to different distresses at different severities. However, because of processing limitations, images are often separated into crack tiles that are processed individually. Depending on the size of these tiles, some information can be lost about crack topology that can be more easily seen from a larger image perspective. Additionally, few methods incorporate crack polygons as a feature, though polygons are the primary component for identifying alligator cracking. Additional research is needed to observe the characteristics of crack polygons and how these characteristics change as alligator cracking forms.

1.2.5 Quantifying Patching Need Using Emerging Technologies

Once potential full-depth patching locations are identified in the field, the volume of material needed to backfill the milled surface is calculated. This volume can be estimated by assuming a constant depth and multiplying by this depth by the total area of patching. This method may result in vast overestimation or underestimation of material

needed, severely impacting labour and costs. To get a better understanding of sub-surface conditions, many agencies will perform core sampling where pavement cores are taken at different intervals to assess sub-surface conditions. This method of sampling is destructive to the pavement and can only give an indication of sub-surface conditions in the area immediately surrounding the core. There is a need to develop a non-destructive method of assessing the depth of pavement distress based on known distress and pavement structure information.

1.3 Conclusion

In the same way that engineers diagnose deep patching need in-field using the surface characteristics, the 2D and 3D pavement images obtained using sensing technology can be processed to show cracking extent and severity throughout a project. The extent and severity results are typically obtained through some combination of projection and Hough transforms, artificial neural networks, and feature extraction. Of these three methods, feature extraction is most emulative of the work done by engineers in the field. This makes feature extraction advantageous as a means of identifying full-depth patching locations from previous crack detection results.

CHAPTER 2. IDENTIFYING FULL-DEPTH PATCHING LOCATIONS USING REMOTE SENSING TECHNOLOGY

The process of identifying full-depth patching locations involves careful planning and labor-intensive work. Inspectors must review the site and manually identify patching locations by walking along the road shoulder and visually inspecting the pavement surface. This time-consuming process can be made more efficient, however, by using emerging technology such as line-lasers which are capable of remotely scanning the pavement while traveling at highway speeds [19]. By using line-lasers to scan the pavement surface, the surface can be quickly captured in high-resolution 3D laser files. These data can then be processed to identify, with high precision, the distresses in the pavement surface. The following chapter proposes a methodology for using high-resolution 3D laser data collected using a Laser Crack Measurement System (LCMS) to identify full-depth patching candidate locations.

Using data collected from US Highway 80 / State Route 26 (US80) near Savannah, GA, a set of pavement images are visually inspected to assess if there is an evident need for patching in the image. This assessment is based on expert opinion given by Ritchie Swindell, a pavement engineer at GDOT, in addition to information collected on-site during full-depth patching operations performed by GDOT. Once the need for patching in each image is determined, images are separated into those requiring deep patching (DP), and images that require no deep patching (NDP). These two sets of images are then processed to detect pavement cracks. The pavement cracking information is used to identify crack characteristics that can be used to classify pavement images, and threshold

values for classification. Threshold values are selected to best identify all DP images, thereby reducing Type II errors and identifying all DP images. Examples of these image types are given in APPENDIX A.

2.1 Sample Data Collection and Validation

Pavement surface data was collected from MP 8 to MP 7 in the westbound direction of the outside lane on US80 in June 2015. The original data set consists of 322 3D laser files, each representative of a 5-by-4.16 m (16.4-by-13.6 ft.) section of pavement. These 3D files were then converted into 2D range and intensity files as shown in Figure 2-1 below.

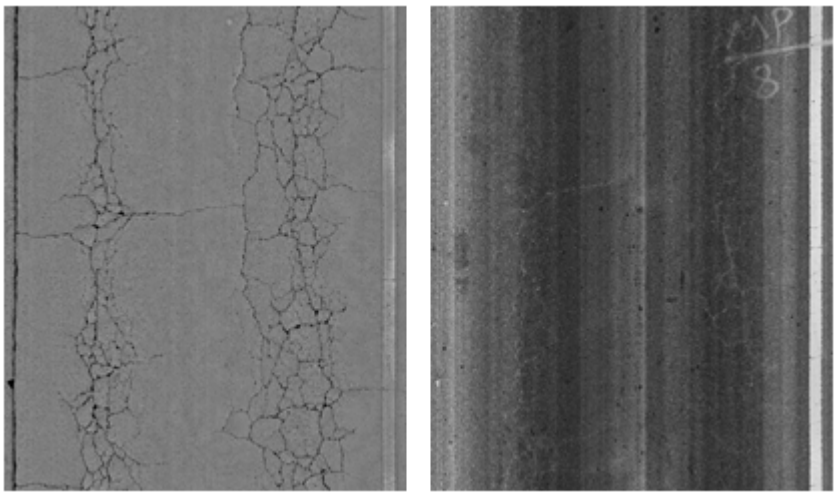

(a) (b)

Figure 2-1 LCMS Processed Images: (a) Rectified Range and (b) Intensity

The two images shown represent the same location; however, the two images show different representations of the surface based on the information recorded by the LCMS. The image on the left uses depth information to show the cracks in the pavement surface and the image on the right represents the reflectivity of the pavement surface. Using the

range images, the all 322 images were assessed with Ritchie Swindell of GDOT to determine a) if the need for patching is evident in either wheel path, and b) if needed, the approximate extents of the pavement patch. This information is validated during on-site trips to US80 during pavement reconstruction, including full-depth patching operations. The information is used to help classify pavement images after distress analysis. Once the need for patching was determined, the intensity images were used to outline the travel lane and the two lane halves.

Using intensity images, the location of pavement striping that identifies the edges of the travel lane in the image is recorded. The locations of the left and right lane markings are used to determine the approximate center of the travel lane. This centerline is used to split the XML data so each half of the lane can be analyzed separately, isolating the two wheel paths. Splitting the original images results in 644 test images, of which 322 are randomly selected to develop threshold crack statistic values for identifying candidate FDP images. The remaining 322 images are later used to validate the threshold values. Before statistical analysis, the images are processed using both automatic and semi-automatic crack detection to establish a ground truth of surface cracking distress. These processes are explained in the following sections.

2.1.1 Automatic and Semi-Automatic Crack Detection

Automatic crack detection is the process of taking pavement surface data, either as 2D images or 3D surface files, and identifying the cracks in the pavement surface using image processing and segmentation. For this study, automatic crack detection was performed using a thresholding and tensor voting algorithm developed by Jiang which

uses image enhancement and a minimal path algorithm [22] to identify crack curves. The images are then transformed using an adaptive thresholding algorithm that generates potential crack maps [23]. This process is shown in Figure 2-2.

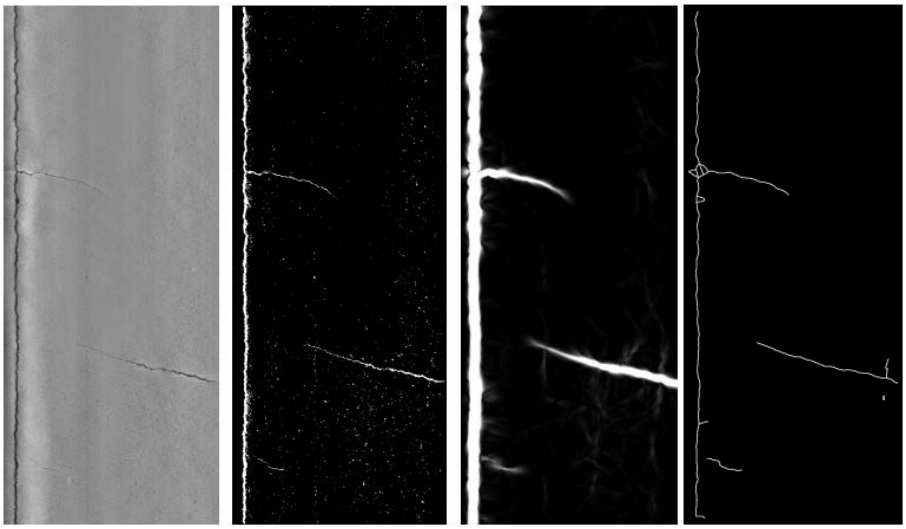

(a) (b) (c) (d)

Figure 2-2 Illustration of Automatic Crack Detection Results

Once these curves are drawn, the images are skeletonized to produce a map of the cracks within the image. The thresholding and tensor voting algorithm gives accurate crack detection results in most cases regardless of lighting and/or shadows that may affect crack detection from 2D images. However, the algorithm may not be sufficient for detecting crack curves in alligator cracking because the cracks are too densely situated for the algorithm to differentiate using thresholding and tensor voting [24]. An example of this is shown in Figure 2-3 where crack detection using thresholding and tensor voting was performed on an image containing alligator cracking.

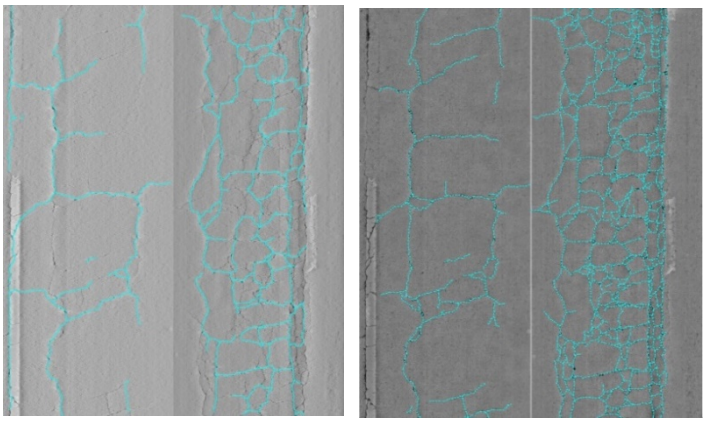

Figure 2-3 Crack Detection: (a) Automatic and (b) semiautomatic adjusted

From the figure, we can see that, although most cracks are detected, many of the smaller, internal cracks are missing resulting in an incomplete detection. To complete the crack detection results, the undetected cracks are drawn on the images using a minimal path algorithm [22] that uses manual input for the start and end points of cracks. This process, referred to as semi-automatic crack detection, allows for the addition of undetected cracks to the pavement image. The cracking information is then saved in an XML file for retrieval and compact storage. In these files, each crack in the image is saved as a set of node XY pairs representing points where the crack changes direction. Through semi-automatic crack detection, the automatic crack detection results are reviewed for quality, and corrected as necessary, thereby establishing a ground truth for pavement condition analysis.

2.2 Candidate Image Identification

The pavement cracking information obtained through crack detection is the basis for distress analysis and identifying images that may require full-depth patching; however, because of the large number of images, it would require heavy processing

power to perform image processing on all images in a project. To limit the time and processing power needed, candidate images are identified based on three characteristics: 1) the total crack length (TCL) in the image, 2) the length-weighted (or average) width (LWW) of the cracking, and 3) the spatial density of crack nodes. These criteria give sufficient information for preliminary classification, but do not require heavy processing power.

The TCL for each image is calculated by summing the distance between adjacent nodes in the XML file where nodes represent X-Y pairs of points that outline each detected crack. Similarly, the LWW is calculated using the measured width at the different crack nodes as well as the distance between adjacent nodes. The crack width at each node is measured using a method previously validated by Jiang [23]. The equation for calculating LWW is given below.

$$Average\ Crack\ Width = \frac{\sum \frac{w_i + w_{i+1}}{2} * l_i}{\sum l_i}$$

w_i = width at node i

w_{i+1} = width at node i+1

l_i = distance between node i and i+1

Crack width is one of the pavement condition indicators used by engineers in the field. As pavement condition worsens, cracks widen allowing more water and foreign materials to enter the pavement structure. Research has shown that pavement cores with cracks wider than 0.2 cm have significantly lower indirect tensile strength in the presence of water [25]. Measuring the average crack width in an image provides more information

about current conditions and susceptibility to precipitation. In comparison, the density of cracking is measured and used as an indicator of the extent of damage done to the pavement.

Crack density is measured using the XY node pairs in the saved XML files. To estimate crack density, the *Y* values of the crack nodes in the XML file are placed into a histogram based on their value. The corresponding histogram splits the pavement image into 20 horizontal bands that half the width of the travel lane and 250-mm (0.82-ft) wide. This width is chosen because it ensures that potential patch areas, typically >2-ft in length, will not be contained within a single band. An example of the crack density measurement is given in Figure 2-4 below.

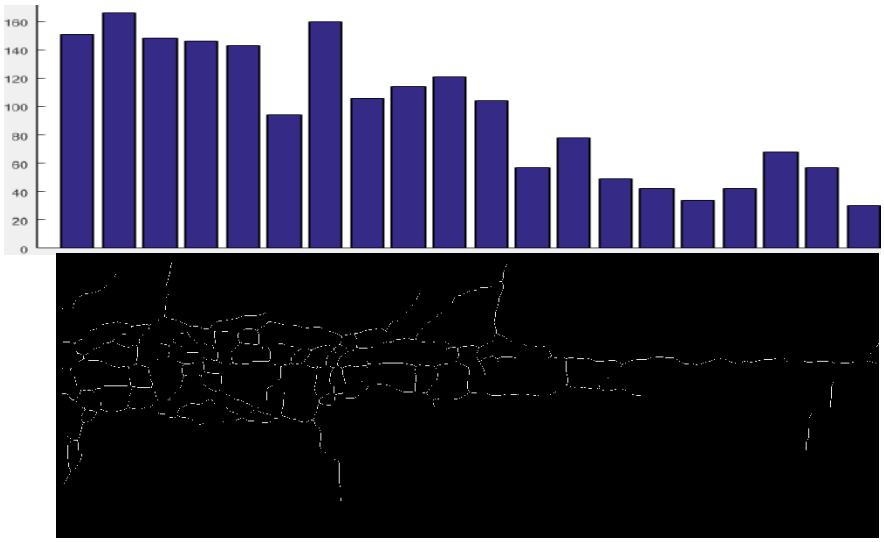

Figure 2-4 Horizontal crack node density histogram

This histogram represents the density of crack nodes for every 250-mm in the driving direction, where the numerous nodes determine the shape of the crack along the surface. As crack condition deteriorates, the density of crack nodes increases and assessing density of DP and FDP images can help develop a crack density threshold. By using a

width of 0.82-ft, potential patch areas, typically >2-ft in length, will not be contained within a single band.

Using the previously observed threshold criteria for TCL, LWW, and density, 322 of the 644 test images collected from US80 were processed to assess the TCL, LWW, and crack density distribution for the images. The images are separated into DP and NDP images per the validated classification by Ritchie Swindell of GDOT. The distribution of distress values in the images is assessed to develop threshold values for quickly identifying candidate images. This method is chosen in lieu of a classifier to reduce Type II error; however, a classifier could potentially be used for this purpose. Various distress value percentiles are given in Table 2-1 below.

Table 2-1 Crack statistic results for classified DP and NDP images

	TCL (m)		LWW (mm)	
Percentile	**DP**	**NDP**	**DP**	**NDP**
0.95	34.17	12.69	30	18
0.9	33.41	11.68	27	17
0.85	30.87	11.17	27	16
0.75	19.51	10.56	20	15
0.5	15.31	8.58	18	13
0.25	13.72	7.122	15	11
0.15	12.43	5.39	15	11
0.1	11.53	4.01	14	10
0.05	10.57	2.22	14	9

From these results, it is determined that a total crack length of 12.2m and a length-weighted width of 14.0 mm are sufficient threshold values for identifying potential DP images. Between 90 and 95% of NDP images have a total crack length less than 12.2 m while 85 to 90% of DP images have a crack length above 12.2 m. Additionally, between 50 and 75% of DP images have a LWW of 14.0 mm or less while all DP images have a measured LWW of 14 mm or greater. Therefore, a LWW value of 14-mm is selected as the threshold for classification. In measuring crack node density, a value of 70+ nodes within a single band is determined to be representative of 95% of DP images. Using these values, potential candidate images can be quickly identified using the cracking XML files, significantly reducing the time and image processing required.

Using these threshold values, the remaining 322 images are classified and compared to validated results to determine the effectiveness of using these crack statistics to classify pavement images. Results are given in Table 2-2 below.

Table 2-2 Image classification results using threshold values

	DP Image	**NDP Image**
DP Classification	32	23
NDP Classification	1	266

Of the 33 DP images, 32 were determined to require full-depth patching using the threshold values. These results indicate that the determined statistics are effective at quickly identifying full-depth patching images using cracking information. The one

incorrectly classified DP image is misclassified because of insufficient length-weighted crack width. The 23 misclassified NDP images are the results of choosing threshold values such that the most DP images can be identified with no false negative classifications. This is done purposefully to ensure all DP images are identified during this process. Given the crack pattern of these images, image processing is performed to eliminate false positive classifications.

2.3 Image Processing to Identify Full-depth Patching Need

To assess pavement topology, the XML files that result from crack detection first need to be transformed into images before processing to assess alligator cracking. For more efficient processing, the XML images used in this study are transformed into binary TIFF images using an application written in C#. In these resultant images, the white pixels represent cracks and the black pixels represent all background information. However, before assessing pavement topology and identifying alligator cracking, the images must first be processed to correct for mistakes that are inherent to the semi-automatic crack detection process.

The semi-automatic crack detection method approximates crack position using manual input. Because of this, the produced crack maps are not as accurate and smooth as automatic crack detection results. This process often results in disconnected cracks that cannot be used for the full-depth patching identification process. To correct for these inherent errors, the images are processed using MATLAB to join cracks and close polygon loops. The steps for image processing are illustrated in Figure 2-5 below.

(a)

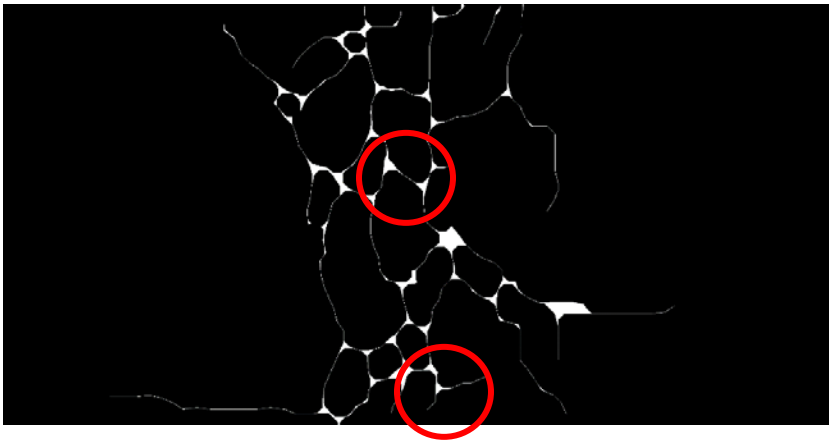

(b)

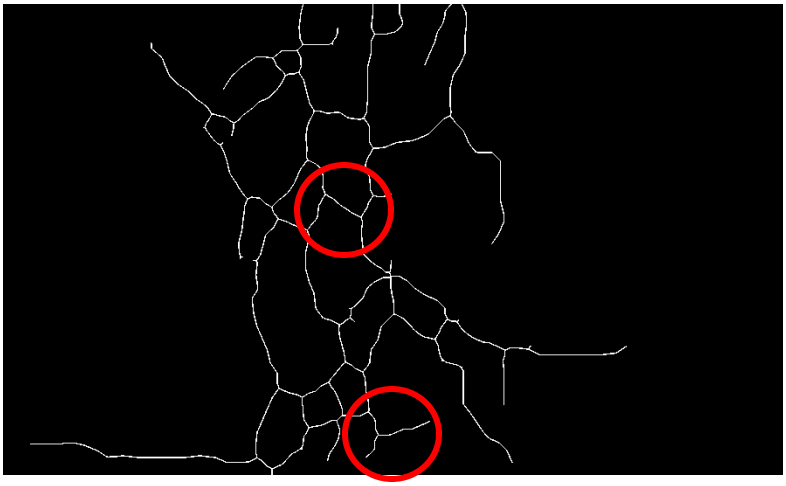

(c)

Figure 2-5 Crack map processing: (a) semi-automatic detection results, (b) image closing, and (c) skeletonization and dilation results

In Figure 2-5, the results of the semi-automatic crack detection process are shown. The circled locations indicate areas in the crack map where the cracks are likely joined; however, due to the crack detection process, the cracks in the resultant image do not join as they should. This is problematic for identification of patching area because the pavement polygons are not closed, and therefore cannot be recognized as polygons by MATLAB. To join crack branches to nearby crack segments and end points, the images are first processed using image closing as shown in Figure 2-5b. Closing the image draws together closely located endpoints and branch points to help make connections.

The images are then skeletonized to reveal the basic crack structure before being dilated to thicken the crack lines. The final result of this process is shown in Figure 2-5c. Through processing, the joining of cracks fully segments the image into pavement cracks and polygons/background. From this binary data, the polygons/background data can be

extracted by inverting the pavement image and identifying the connected components of white pixels.

2.4 Image-level Identification Using Crack Topology

Crack topology, for the purpose of this study, refers to the physical arrangement of pavement cracks and how they connect on the pavement surface. The topology for DP images contains significantly more cracking in addition to polygons formed on the surface from the connected crack. These polygons are the basis for alligator cracking and are indicative of significant base layer deterioration. As the base layer deteriorates, the distresses are reflected to the surface where polygons form as the surface layer crumbles. The degree of crumbling is reflected by the size, number, and spatial organization of polygons seen on the surface. To identify the polygons, the images are inverted to produce images where the active, polygon pixels are white and the crack pixels are black. The connected white pixels are then identified using MATLAB as shown in Figure 2-6a below.

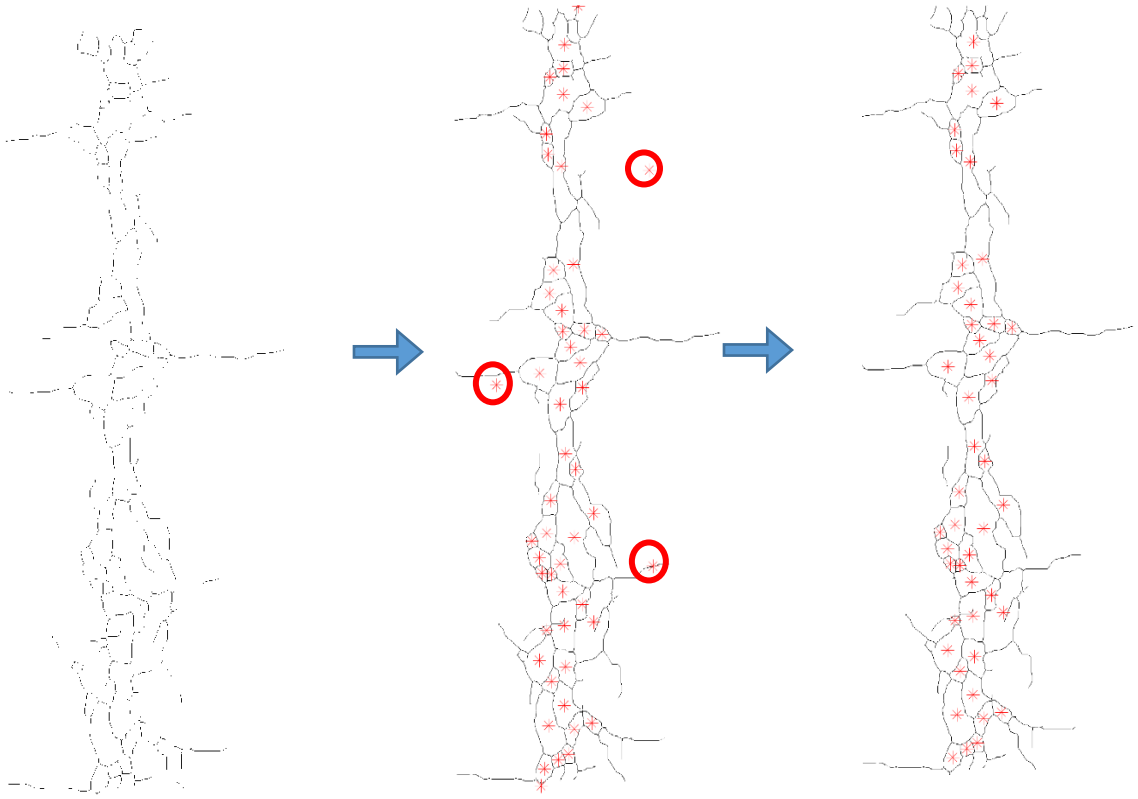

(a) (b) (c)

Figure 2-6 Polygon identification and centroid filtering

After inversion, a MATLAB function, 'bwconncomp', is used to identify the polygons in the image [26]. The name of the function is shortened from 'black and white connected components' and the function is used to find collections of connected white pixels in a black and white image. Once identified, the centroids for the polygons are plotted as shown in Figure 2-6b. Connected components in the center and the edge of the image that are outlined by cracks in the wheel path are removed because they are not indicative of the pavement condition in the wheel path. Once the polygons in the wheel path are identified, the centroids are clustered to identify the extent of patching in each image.

2.4.1 Polygon centroid clustering to form patches

The method used to cluster polygons is a distance-based algorithm that clusters any two polygon centroids if they are within a certain maximum distance of each other. Additionally, a minimum number of centroids (MNC) within a cluster is set to avoid small clusters of polygons. Clustering results for two images are given in Figure 2-7.

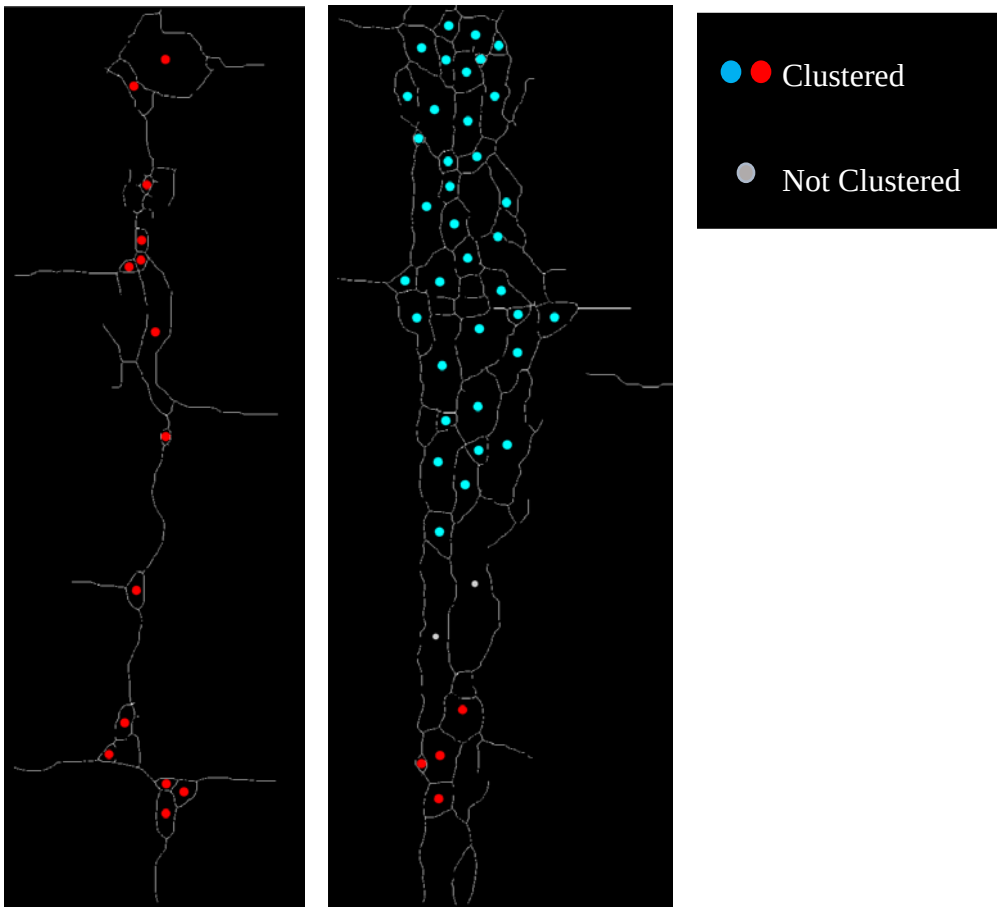

Figure 2-7 Polygon clustering results a) large spacing, b) unclustered polygons

Different centroid clusters are highlighted by different colors while grey centroids indicate polygons that are not assigned to a cluster due to spacing. The maximum spacing to cluster two nodes, referred to as the maximum centroid distance (MCD), in a cluster is set as 711-mm (2.33-ft). To determine the optimal maximum centroid distance and minimum number of centroids to form a cluster, a test is performed. Using four different MNC values ranging from three to six and seven MCD values ranging from 305-mm (1-ft) to 914.6-mm (3-ft). All combinations of MNC and MCD values are processed and the results are reviewed to determine which values best match the validated full-depth patching results. Several examples are given in Figure 2-8.

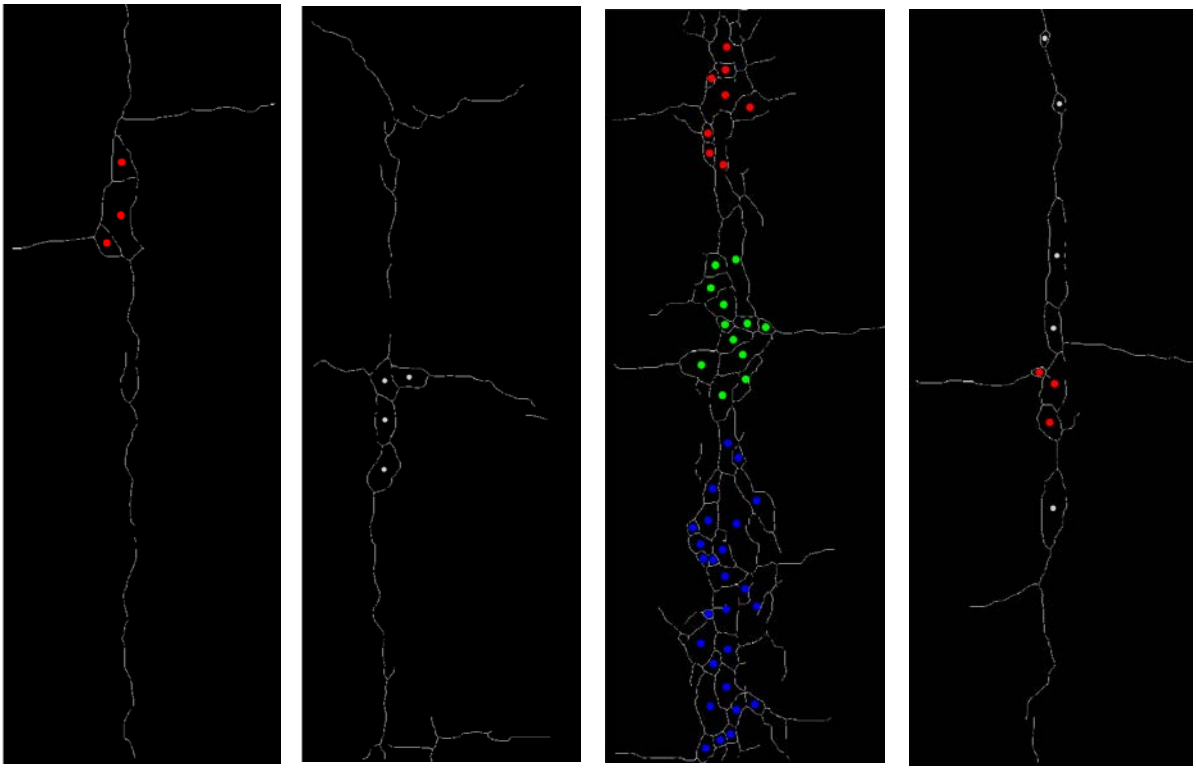

Figure 2-8 MNC and MCD Tests: a) MNC = 3, b) MNC = 6, c) MCD = 305-mm, and d) MCD = 915-mm.

The values chosen for MNC and MCD are selected to mimic the results from the validated test images. Extreme MNC values, as shown in Figure 2-8. (a) and (b), may not capture the adequate size for patching identifying patches that are too small or cracking that is not severe enough to warrant full-depth patching. Likewise, extreme MCD values may not cluster centroids properly, resulting in too many clusters in one image or clusters that are disconnected from adjacent polygons as shown in Figure 2-8. After the polygon centroids in the images are clustered, the longitudinal limits of the polygons in each cluster are used to determine the termination points of the pavement patch. Typically, engineers place a 1-ft boundary around the affected area to ensure all damaged pavements are successfully removed. Patches that are shorter than 610-mm (2-ft) in length are removed because they are unlikely to be patched due to the limited size of the patching equipment. Once the shorter patches are removed, a 1-ft boundary is added to the affected area. This is to mimic the procedure performed by engineers in the field. The additional boundary helps ensure the entirety of the damaged pavement is removed.

After removing small patches, the remaining patches are clustered based on their linear spacing. In practice, if two patching locations are in close proximity, it is likely that they will be identified together as one patch and both are excavated as well as the area between them. After talking with pavement experts at GDOT, the minimum distance between patches is estimated at around 4-ft (~1220-mm). Any patches within this short distance are identified and assessed as a single patch. This gives the final full-depth patching analysis results for the given set of images.

2.5 Conclusions

The proposed method is validated using a set of 322 test images with known need of full-depth patching in each image. After reviewing the images, threshold TCL, LWW, and crack density values are selected to use to classify pavement images. These threshold values show promise for identifying FDP images using basic cracking information. The threshold values are selected to identify all possible full-depth patching images; however, they can be easily altered to adapt to different distress protocols. Because the threshold values are selected to identify all FDP images, there are a significant number of false positive classification results. These are removed using image processing.

The candidate FDP images are processed to identify the polygons formed by the cracking. The centroids are then clustered based on distance. It is determined that, to best follow the ground truth classification, centroid clusters must have at least four centroids, all of which are within 711-mm (2’4”) of at least one other centroid. These MNC and MCD values are estimated from a small set of test data; however, they can easily be altered based on the needs of different agencies and how they define alligator cracking. The method shows strength in the identification of full-depth patching locations based on crack topology.

CHAPTER 3. ANALYZING PAVEMENT CORES TO ESTIMATE PAVEMENT DISTRESS DEPTH

To evaluate the proposed method and identify the subsurface characteristics of distressed pavements in need of full-depth patching, a study is performed compare the condition of pavement cores taken from different locations with what is seen from the surface. The pavement cores included in the study were collected in February 2016 on US80/SR26 near Savannah Georgia. The 4" diameter cores range from 4.5 to 14.5 inches in length and all contain cracks from which crack width and depth are measured. Additionally, the pavement structure from which the cores are taken is typically 1-2" of HMA surface course and ~5-5.5" of HMA base. The thickness of these layers helps determine the strength of the pavement structure and how resilient it is to breakage between layers or crumbling due to heavy traffic loads.

The cores are then classified as intact, broken, or crumbling based on their condition. Of the 13 cores, seven are classified as being *intact* (I) while the remaining six are either *broken* (B) or *crumbling* (C). Intact cores have remained as a single piece, broken cores show separation between pavement layers, and crumbling cores have broken into multiple pieces with no discernable pattern. Examples of different core conditions are shown in Figure 3-1. Additional pavement core images can be found in APPENDIX B.

(a) (b) (c) (d)

Figure 3-1 Core conditions: a) broken, b) crumbling, c) soil, and d) intact

Each core is visually inspected to assess characteristics relating to condition including: 1) depth of cracks, 2) width of cracks (both maximum (MCW) and an estimated representative (RCW) width), 3) separation of layers, and 4) presence of soil in the cracks. The locations of the representative and maximum crack widths are visually estimated. Cracking and soil results from the 13 cores are given in Table 3-1 below.

Table 3-1 Coring Study Results

ID	Soil	RCW (mm)	MCW (mm)	MCD (cm)	Core Depth (cm)	Classification
C4	N	10	12.5	28	22	B
C5	N	1	2.5	7.5	22	I
C6	Y	7.5	12.5	16.5**	16.5	C
C7	N	1	2	11	20	I
C8	Y	2.5	5	18**	18	C
C9	N	5.5	10	5	22	B
C10	N	2.5	5	8	23	I
C11	N	1	2	6.5	22	I
C12	Y	1	2.5	28**	N/A*	C
C16	N	0.5	1	8	18	I
C18	N	2.5	3	16.5**	16.5	I
C19	Y	3	7.5	7.5	15	C
C21	Y	N/A*	10	N/A*	11	C

* Value could not be adequately measured because of poor core condition

** Crack depth is equal to core length but may extend beyond depth of core

Crack width, crack depth, and the presence of soils in the core are important for determining the severity and extent of deterioration of the pavement below the surface. As condition deteriorates, cracks widen and deepen. Additionally, bottom-up cracking begins to occur which allows for the finer, sand material from the subgrade to migrate

upwards towards the surface. These characteristics are good indicators that the pavement is no longer able to sustain the traffic loads being applied and is beginning to deteriorate quickly. The proposed method is validated using the cores as references for sub-surface conditions.

3.1 Validating the Proposed Method using Asphalt Pavement Cores

The proposed method seeks to identify alligator cracking and locations with poor load-carrying capacity. These locations are characterized by pavement that is crumbling not only in the surface layer, but also in the layers beneath. Additionally, as asphalt material is washed away by water, soils and other fine materials migrate from the subgrade into the newly formed cracks, resulting in severe soil deposits. The combination of fine soil material and crumbling characteristics are present in five of the 13 pavement cores. Because of their deteriorated condition, it is clear that the location surrounding these five cores would require full-depth patching. Therefore, these cores can be used to validate the proposed method's ability to identify patching locations.

To validate the proposed method, the 3D laser system is used to scan the pavement surface from which the cores are taken. After collecting the pavement images, the cracks in the images are identified using semi-automatic crack detection and the images are processed per the proposed method. The resultant patching need within each image is compared with the location of pavement cores to determine if the five crumbling cores are correctly identified as requiring patching. Results show that of the 13 cores used in the study, the five cores with soil material and classified as *crumbling* are correctly identified by the proposed method. From this method, the area in each image that

required full-depth patching is detected. Examples of these detected full-depth patching areas are given in Figure 3-2 below.

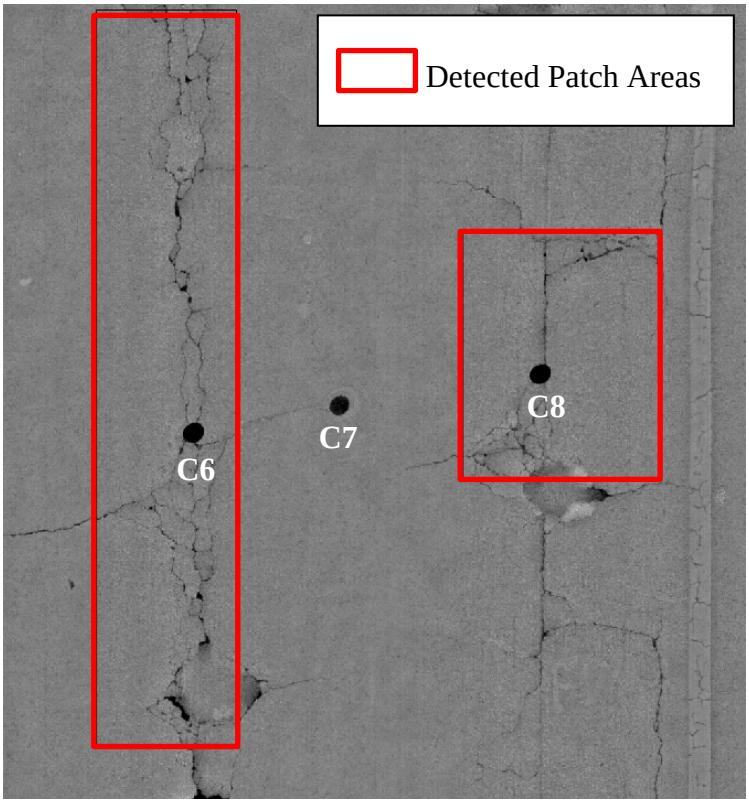

(a)

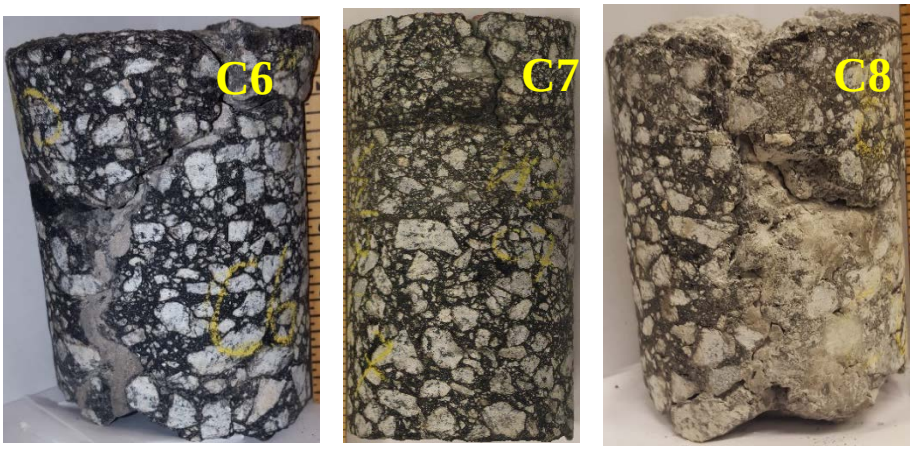

(b)

Figure 3-2 Cores C6, 7, and 8 Validation – a) Detected patching, and b) Cores

From Table 3-1 it is observed that cores C6 and C8 both exhibit crumbling and contain soil material while C7 does not. This is confirmed from images of these three cores, given in Figure 3-2b. The conditions of these three cores directly reflects the results of the proposed method given in Figure 3-2a. The two crumbling cores with soil present are identified in the patching extent while the remaining core, C7, is not within patching limits. Similarly, the remaining three pavement cores classified as crumbling and containing soils are identified by the proposed method. Results can be found in APPENDIX C.

The image suggest that the proposed method shows promise for identifying areas with severe base problem. All cores classified as *crumbling* are identified as requiring patching while all other cores were located outside of the patching area. This suggests the condition of the base and subgrade layers in the pavement can be qualitatively assessed from the surface. However, to fully assess patching need, quantitative estimates must be made to determine the depth of pavement distress.

3.2 Correlating Surface Condition with Pavement Core Condition

Of the 13 cores used in this study, five are classified as crumbling due to severe distress. These cores typically have cracking for the full depth of the core and show soil material in the bottom-up cracking in the core. The severity of the distress seen within the core is expected to reflect to the surface as alligator cracking. To correlate the surface distress with the condition of the core, the 3D pavement data is used to measure the condition of the pavement immediately surrounding the pavement cores. Using manual input, the location of each core within the image was recorded. Using this location, the

cracking data in a 4-by-4 ft. (1.2-by1.2 m) bounding box around the core was taken. The *total crack length,* and *length-weighted width* in this bounding box are measured for each core.

3.2.1 Measuring crack density and length-weighted crack width in a bounding box

In this study, crack density is measured as the total crack length within the 16-ft^2 (~1.5-m^2) bounding box around the core. Using MATLAB, the location of the cores in the pavement images are given as input and the TCL and LWW in the bounding box are calculated from the XML data. Results of this study are given in Table 3-2 below.

Table 3-2 Crack Density and Length-Weighted Width in Bounding Box

ID	Crack Density (m)	LWW (mm)	Classification
C4	0.79	15.6	B
C5	1.25	15.9	I
C6	7.22	18.6	C
C7	2.33	12	I
C8	6.63	19.8	C
C9	1.37	11.1	B
C10	1.62	6.9	I
C11	0.99	8.3	I
C12	4.32	14.7	C
C16	0.54	12	I
C18	2.52	11.9	I
C19	5.49	18.5	C
C21	18.3	14.7	C

Of the 13 cores used in the study, all five cores classified as ‘crumbling’ have a high crack density ranging from 4.3-m to over 18-m. All cores classified as ‘broken’ or ‘intact’ have a much lower crack density, ranging from 0.5-m to just over 2.5-m. This disparity in crack density measurements indicates that crack density can be used to qualitatively assess pavement conditions in terms of material crumbling below the

surface. Results indicate a total crack length above ~4.0-m in the bounding box is indicative of crumbling beneath the surface. Because it is a good indicator, density is used to assess the correlation between surface characteristics and crumbling.

3.2.2 Assessing changes in crack width with increasing crack depth

To quantitatively assess pavement condition, the width and depth of cracking in the pavement cores are compared against the crack density measured in the surface. Crack width is indicative of the susceptibility of the pavement to water damage while crack depth is indicative of the loss of strength of the pavement layers. These pavement characteristics are important for determining the remaining life of the pavement, and the need for full-depth patching.

For each of the cores in the study, the length-weighted width was calculated in addition to measuring the estimated representative and maximum crack widths on the core surface. In several cases, the pavement cores exhibited spalling, the breaking away of material around a pavement crack or joint. This was primarily present on pavement cores classified as broken or crumbling. For this study, crack widths were recorded according to FHWA guidelines [27]. With this technique, the pavement spalling is not measured as part of the crack width as illustrated in Figure 3-3.

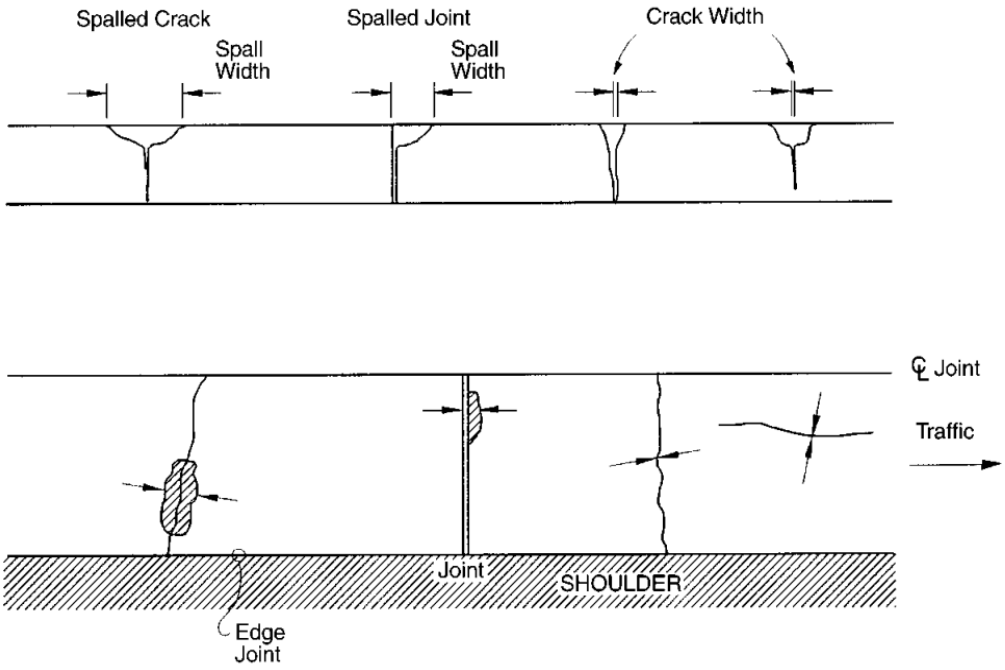

Figure 3-3 FHWA Spalling Crack Width Measurement [27]

For pavement cores classified as crumbling or broken, crack widths are estimated. Because the cores have broken into multiple pieces, the correct crack width could not be measured, and was therefore estimated by reassembling the pavement core pieces and measuring crack width from the reassembled core. After measuring the representative and maximum crack widths on the core, the width values as well as the LWW from cracking around the core are compared against the density of cracking around the core as shown in Figure 3-4.

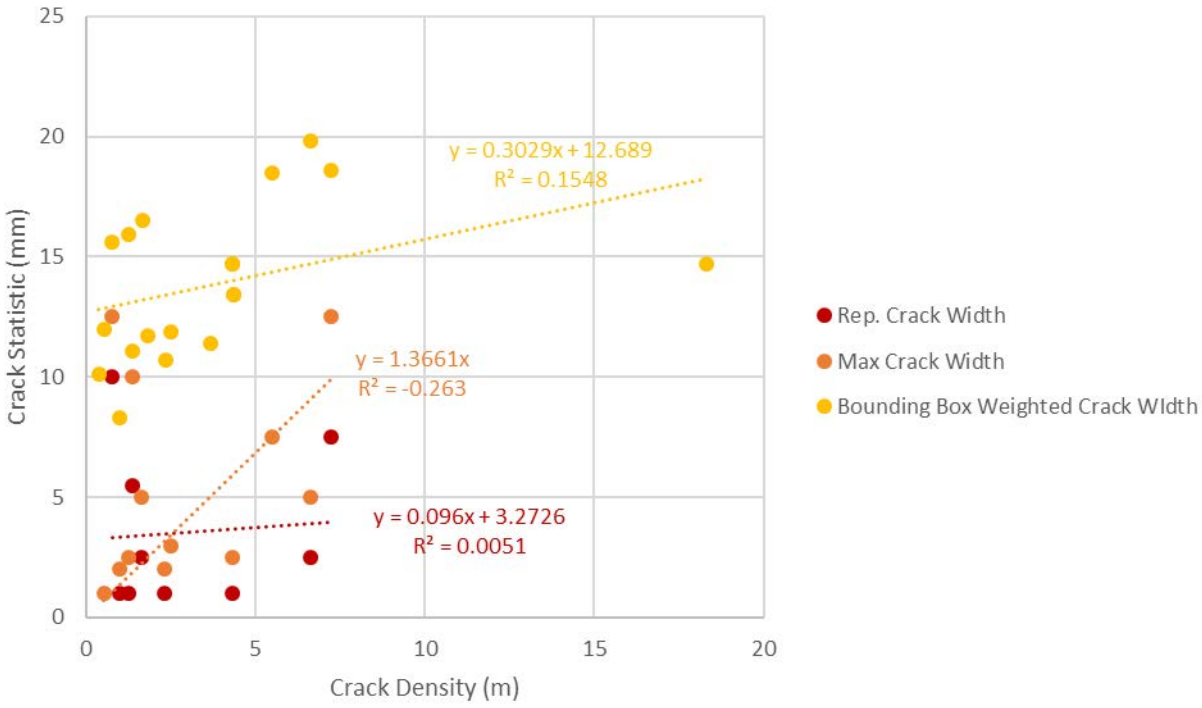

Figure 3-4 Length-Weighted Width v. Crack Density

From the figure, it is observed that the measured representative and maximum crack widths do not strongly correlate with the crack density around the core. This is likely because of the inherent bias in measuring representative and maximum crack width. In contrast, the LWW calculated from the XML files shows a noticeably stronger correlation with the crack density. This suggests that, rather than looking at an individual location, the condition below the surface at a point can be best estimated using the immediate surroundings. To further explore this idea, crack depth for each core is compared to the crack density in the surrounding area.

The measured maximum crack depth from the cores can be used as a baseline to determine the approximate depth needed for patching in areas with alligator cracking. For these areas, the crack depth is assumed to be constant, whereas for areas with low

severity cracking, the depth is more likely to vary. This maximum crack depth is expected to increase as the measured surface cracking density increases. To assess the correlation between crack depth and crack density, the measured density is plotted against the maximum measured depth. For the crumbling cores, C21 was removed from the dataset because of the extreme crack density. All other cores are plotted in Figure 3-5.

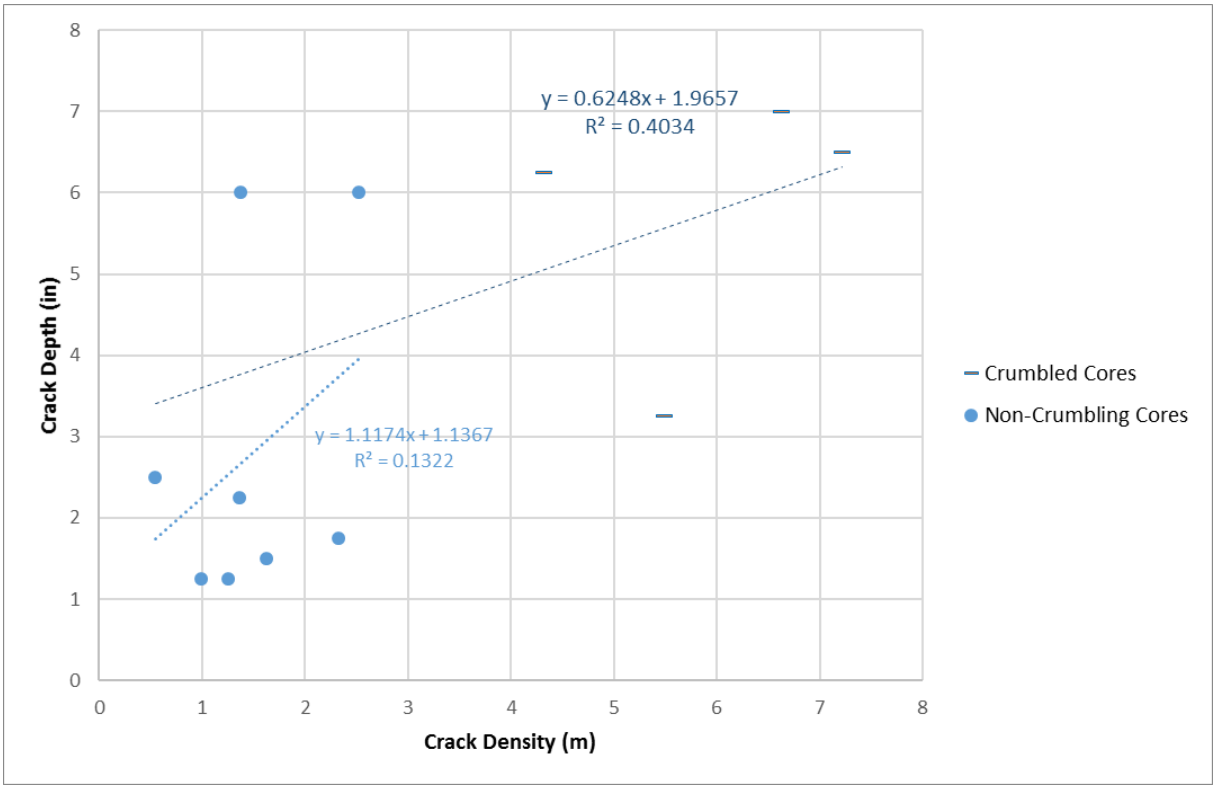

Figure 3-5 Crack depth v. crack density

The longer regression line shows the correlation between crack density and crack depth when including all pavement cores. The crack depth for these cores is taken as the full height of the core although the depth of distress at that location is likely much deeper than the height of the core. This is due to the limitations of the drilling equipment when sampling cores. Including all cores, there is significant correlation between crack depth

and the density of surrounding cracks. However, the variability of the data makes it difficult to make meaningful estimations of the depth of distress using only crack density.

Because the crumbled cores have a higher surrounding crack density, they lie further to the right on the graph. The large disparity between crumbling and broken/intact cores limits the certainty of the depth measurements given the limited data size; however, the data is useful for assessing special cases that may help give more insight into what may cause rapid deterioration. For the broken and intact cores, crack depth is consistently above 3-in, while for crumbling cores, the depth is typically below 3-in except for in the cases of C4 and C18.

Core C4 has a measured crack density of just 1.372-m in the surrounding area which is comparable to the average of 1.518-m for other non-crumbling cores. Although the crack density is comparable to other similar cores, the LWW of C4, 15.6-mm, is more comparable to cores classified as crumbling (average LWW is 17.6-mm). From

Table 3-1 it is also observed that C4 has the highest representative and maximum crack widths of all pavement cores. Images of the core and surroundings are given in Figure 3-6.

(a) (b) (c)

Figure 3-6 Pavement Core C4 - (a) Top, (b) side, and (c) surroundings

The high crack width measurements and severe breaking between pavement layers suggest that the pavement structure was degraded by water infiltration. Because the crack is so wide, water can easily infiltrate the pavement structure and erode the material; however, because there is only one crack, the deterioration of the pavement is likely slowed compared to areas with higher densities of cracking. The singular, wide crack allows water to infiltrate and erode the one crack, but lack of adjacent cracking slows the deterioration of the area. Considering the low crack density, the depth of distress is higher than what would be expected, as is the crack width.

In addition to C4, C18 has an unusually high crack depth for the surrounding crack density. This core, shown in Figure 3-7 below, has a low crack width and minimal spallin2g, but the crack extends to the full depth of the core.

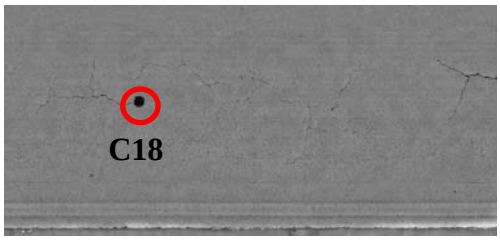

(a)

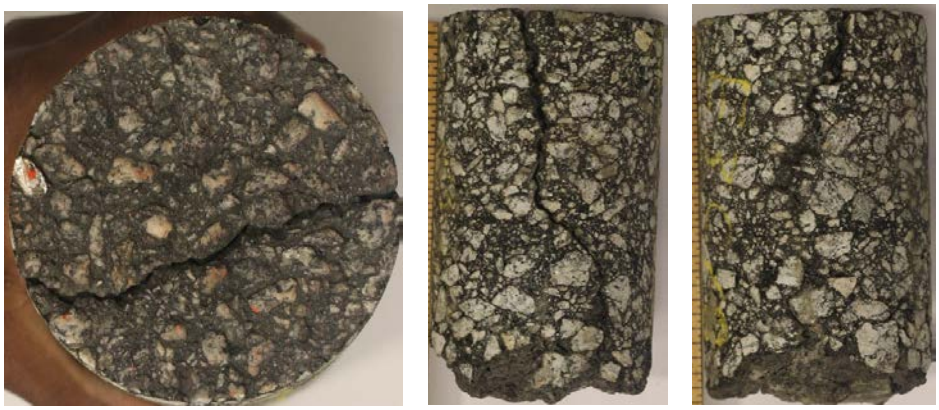

(b) **(c)** **(d)**

Figure 3-7 Pavement core C18

Although the crack penetrates through the full length of the core, the crack behaves differently on the two sides. On one side, pictured in Figure 3-7a, the crack width is constant through the top layers and begins to change direction and narrow in width in the bottom layer. Contrarily, on the other side, the crack is wide at the top of the core and visibly changes width as it propagates through the top pavement layers. The behavior of crack width through the layers may indicate an issue inherent to the materials and bonding of the layers. This may indicate why the crack depth is significantly higher than expected given the surrounding crack density.

Because crack density is easily measurable from crack detection results, it is a suitable method for assessing sub-surface conditions. From this study, crack density is shown to have some correlation with the weighted crack width of an area. The weighted crack width is indicative of the permeability to water, and by associating this width with crack density, more is understood about the deterioration of pavement in water-prone areas. Crack depth is shown to have some correlation with crack density; however, the variability within the small sample size limits the ability to adequately estimate the depth of distress. Although more information is needed to make predictions about crack depth from surface conditions, conclusions can be made from the assessed pavement cores.

From this study it is determined that pavement with crack density >4.0-m, are likely to show severe crumbling that extends through the surface and base layers and typically extends more than 6-in. into the pavement. Traditionally, pavement engineers at the Georgia Department of Transportation use a milling depth of 4” as a standard for full-depth patching. This study suggests this depth may not adequately cover the full extent of distress in the pavement layers, leading to problems in the future.

3.3 The Importance of Adequate Patch Depth Estimation

When performing full-depth patching, removing material to the correct depth is equally as essential as identifying the correct locations for patching. Once the defective material is removed, the milled surface serves as the base for the asphalt material used as filler. If this base is unstable or defective in any way, the foundation is no longer solid and the new surface will deteriorate much more quickly. The images in Figure 3-8 were

taken from US Highway 80 near Savannah, Georgia after the top four inches of pavement were milled as part of a full-depth patching procedure.

(a)

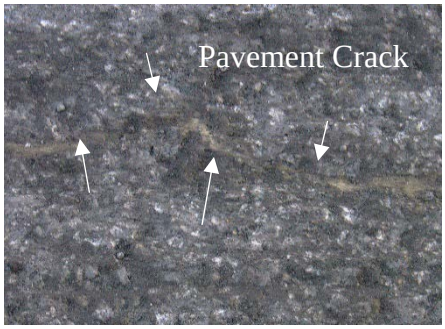

(b)

(c)

Figure 3-8 Cracking and crumbling on 4" milled surface

For this project, GDOT was performing full-depth patching procedures for both directions of the roadway before performing a 1-in. resurfacing. The 4-in. milled surface for full-depth patching is shown in Figure 3-8a and the other two figures show close-up views of the surface. In several cases for the patching, upon further inspection, cracks were still visible in the 4-in. milled surface (Figure 3-8b). In some cases, the surface even showed severely broken/crumbling material (Figure 3-8c). These defects can weaken the structural integrity of the roadway and are likely to lead to similar problems in the future.

3.4 Conclusions

The cost, labor, and materials for resurfacing and repair projects rely on engineer judgement and recommendations of how to best treat pavement while remaining within an allotted budget. Because it is time-consuming and labor intensive, full-depth patching is one of the major components to the budget and the more information that is known about the need for patching, the more efficiently the project can be carried out. Current methods of estimating the depth required for patching, or using a constant depth are largely based on engineer experience which may be subjective and can lead to underestimation of patching material which extends the time and labor required for patching.

Using the proposed method, these areas can be identified from the detected crack data and quantified in terms of area. This can potentially save engineers and inspectors significant time in the field that is typically spent performing inspections. The proposed methodology also helps give more information about the topology of alligator cracking which can be used to assess how deep the distress is into the pavement.

Traditionally, pavement cores are used to determine the depth of pavement distress; however, emerging sensing technology is shown to be useful in assessing how the cracking topology correlates with depth of pavement distress. By assessing pavement cores and the surrounding cracking condition as measured using sensing technology, more can be understood about the subsurface conditions. Of the 13 cores used in this study, the five categorized as crumbling all have a surrounding crack densities above 4.3-m while the densities of non-crumbling cores is consistently below 2.3-m. The large

difference in density measurements of the two categories suggests crack density is a good standard for assessing pavement condition. Because of this, crack density is used as a baseline for comparing crack width and depth measurements for the two categories.

Although crack width is not used when identifying full-depth patching locations, it is useful for assessing pavement condition and determining the susceptibility of a location to water damage. For each core, the maximum surface crack width, representative width, and the surrounding LWW are compared. Although representative and maximum crack width do not show much correlation, the measured LWW for crumbled cores average 17.3-mm with a standard deviation of 2.1-mm while the average LWW for non-crumbling cores is 11.7-mm. with a standard deviation of 3.1-mm. Although the sample size is small, LWW shows correlation with cracking density which is strongly indicative of the need for full-depth patching.

For locations with little to no remaining life and severe structural damage, it may be difficult to initially estimate the distress depth. To analyze the effects of structural damage, thirteen cores were analyzed to see how crack depth/ distress depth changes with crack density. For the five cores classified as crumbling, the crumbling nature of the pavement caused the cores to fall apart such that the actual distress depth cannot be adequately measured. For these cores, the distress depth is assumed as the full depth of the core (typically >6”). When looking at distress depth for crumbling cores, four of the five cores have a distress depth above 6.25-in. For non-crumbling cores, all but two of the eight measured distress depths are less than 2-in. There is a clear increase in depth of distress for the two categories of cores; however more information is needed to understand the surface conditions of pavement with distress depth that is between 2 and

6.25 in. Through this analysis it is shown that there is a correlation between crack depth and crack density, however results are not conclusive enough to estimate depth of distress by solely using crack density.

CHAPTER 4. CASE STUDY: A TEMPORAL ANALYSIS OF FULL-DEPTH PATCHING NEED ON US80/SR26

Using the proposed method, the growth of patching need can be identified over time as a segment of road is left to deteriorate. By looking at the need for patching across multiple years, the data can be analyzed to identify areas that appear to deteriorate faster than other locations subject to similar traffic and weather conditions. Although the traffic along the roadway may be virtually consistent, certain areas may be more prone to distress based on issues related to either construction or the roadway environment. By analyzing temporal data, the increase in patching need for the road can be quantified and assessed to determine the reasons for growth. Areas with accelerated deterioration can be identified and a field investigation can be performed to determine the cause of the accelerated deterioration.

In this chapter, a segment of US80/SR26 near Savannah, GA is analyzed to estimate the need for patching across multiple years using the proposed method. The road is divided into 100-ft and 200-ft segments and the need for patching in each segment is analyzed across multiple years to determine the increase in patching need for all segments.

4.1 Data Collection and Processing

3D pavement surface data was collected from US80 for 3 timestamps between December 2011 and June 2015. US80 is a major state highway with an estimated Annual Average Daily Traffic (AADT) of 19,200 in 2016 with 12.08% truck traffic [28]. The

route, shown in Figure 4-1, serves as a connector of Pooler, GA, I-95, and the coastal area.

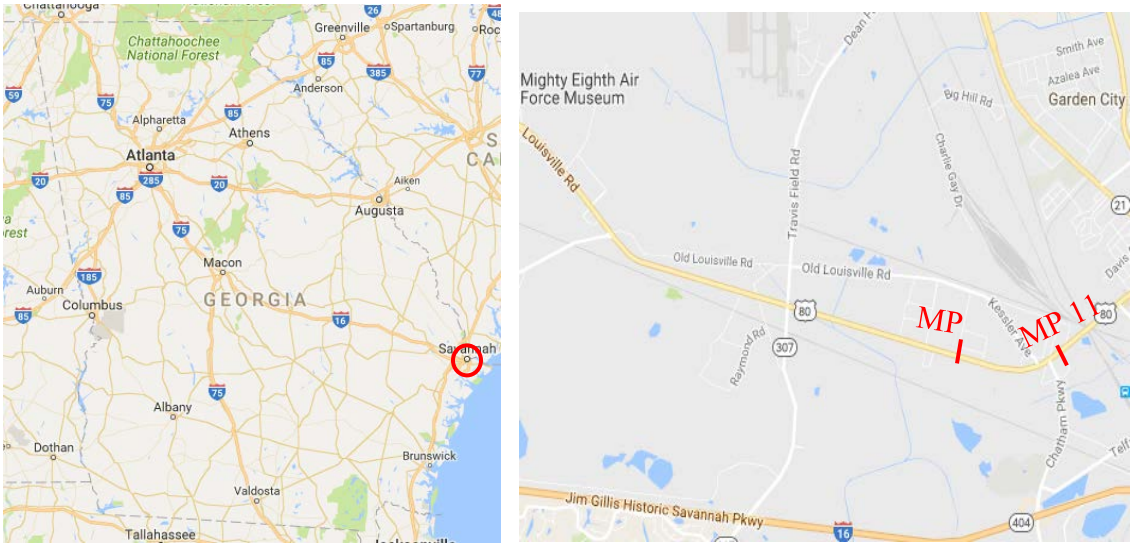

Figure 4-1 Map of US80/SR26 near Savannah , Georgia

The data collected is from MP 10 – 11 in the EB direction. This section is identified as having a range of pavement conditions including severe alligator cracking in multiple locations. The wide variety of pavement conditions allows for comparison of the deterioration rate of pavement initially in good to fair condition against the deterioration rate of pavement that begins in poor to failing condition. Information on the data collected is included in Table 4-1.

Table 4-1 3D Laser Image data for Temporal Study

Data Collection Data	No. Laser Files
2011/12/06	325
2013/12/07	326
2015/06/15	326

The number of laser files indicates the total number of files collected; however, for the analysis each image is separated into the left and right lane sides for patching analysis. Using the pre-determined lane markings, the location of the lane center is used to split the image so the left and right lane sides can be processed separately. Additionally, the lane markings are used to identify locations where the travel lane is not fully covered by the width of the sensors due to transverse movement of the vehicle.

4.1.1 Correcting for vehicular wandering

The slight difference in the number of laser files is inherent to the driving behavior of the van operator. By not driving in a straight line, the van does not travel the exact same distance across different years. This results in a lack of full lane coverage as shown in Figure 4-2.

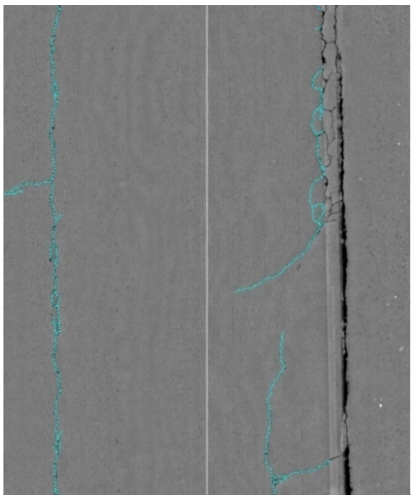

Figure 4-2 Poor lane coverage due to vehicular wandering

Because the vehicle traveled too far to the right, part of the left lane is no longer covered. Because of the vehicle's position, some of the cracking in the left lane side is not covered, possibly resulting in improper classification. To correct for this, the one mile used for this study is separated into 29 segments. The first 400-ft are divided into ~100-ft segments, and the remaining length is divided into 24 200-ft segments as well as a final 80-ft segment. This is done by identifying significant cracks/distresses that are recognizable across all timestamps and marking these locations across all years. By using these reference locations throughout the mile, the impact of vehicle wandering is minimized through the intermediate stations.

Because of wandering, the cracks in some sections are not covered in all years. These images are identified using the lane markings. For all segments across all years, if any of the images within the segment do not cover the full lane width, the segment for that timestamp is not included in the study. The number of removed sections is outlined in Table 4-2.

Table 4-2 Vehicular Wandering Missing Sections

	Left Lane Side	Right Lane Side
2011	9	0
2013	3	0
2015	3	0

Vehicular wandering is primarily an issue for the 2011 results in the left half of the lane. Therefore the need for patching in the left lane is for this year is likely inaccurate. The right lane is fully covered for all years across all three timestamps. After the images are divided into the left and right lane sides and the locations without full lane coverage are removed, the patching need for each mile is determined across different timestamps.

4.2 Patching Need on US80 MP 10 – 11

After determining which locations did not have full lane coverage for the three timestamps, the total amount of patching in each section was measured for all three years. Because there were no major reconstructive projects between the first and last collection date, the amount of patching is expected to significantly increase in the four-year span being observed. Results of the total patching need estimation are given in Table 4-3.

Table 4-3 Estimated Patching Need for US80 2011 - 2015

	Number of Patches		**Total Patch Length (m)**	
	Left	*Right*	*Left*	*Right*
2011	6	8	8.58	21.7
2013	26	27	136.96	209.95
2015	27	31	240.32	338.3

There is a clear trend of growth for both the left and right wheel paths; however, the amount of growth between 2011 and 2013 for the left lane side is likely exaggerated due to the nine sections that are not covered because of vehicle wandering. The right wheel path, however; is fully covered in all timestamps, indicating significant damage was done to the pavement in the two years between collections. From 2013 to 2015, the growth of patching need is smaller than the previous two years, but there is still a significant increase for the left (75.6%) and right (61%) lane sides.

To better understand the distribution of patching need within the one-mile segment, the individual 100 and 200-ft segments are analyzed separately. Through this analysis, the growth in each section is measured to determine which segments have the highest patching need as well as which segments are deteriorating the fastest. This will help develop a better understanding of what may be causing these segments to deteriorate so quickly compared to other segments. Results from this analysis are given in Figure 4-3 below.

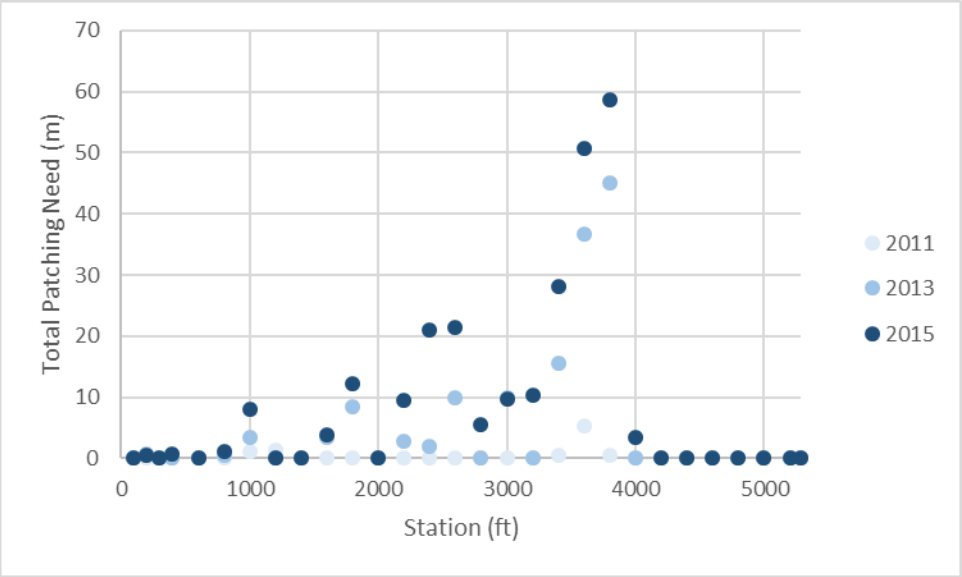

(a)

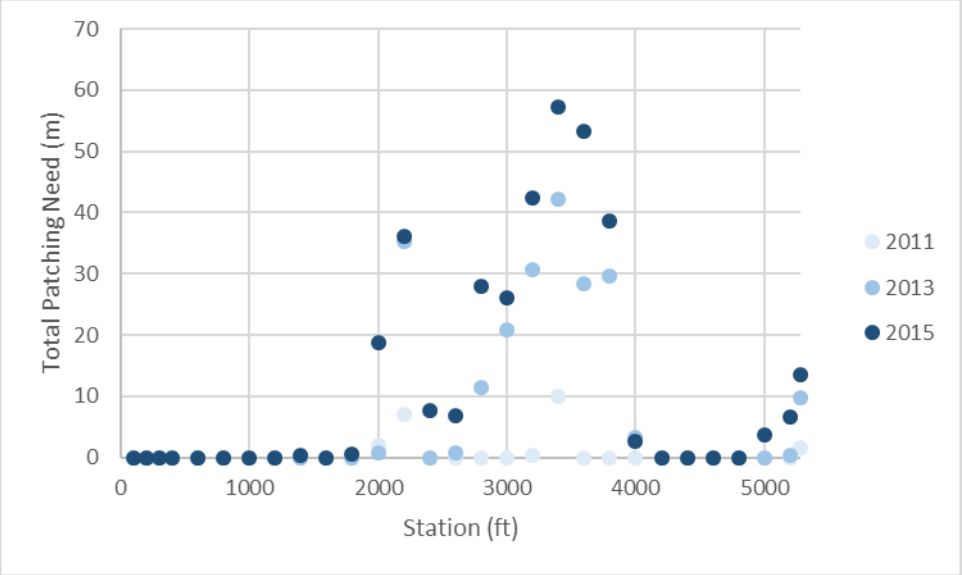

(b)

Figure 4-3 Full Depth Patching need on US80 from 2011 to 2015 a) Left lane side, b) right lane side

From the figure, it is observed that, for both sections, most full-depth patching need occurs between stations +2000 and +4000 for both lane sides. Additionally, for the right

lane side, there is a noticeable increase in patching need towards the end of the mile. To better understand the changes between years, the difference in patching need for the 29 segments is given in Figure 4-4.

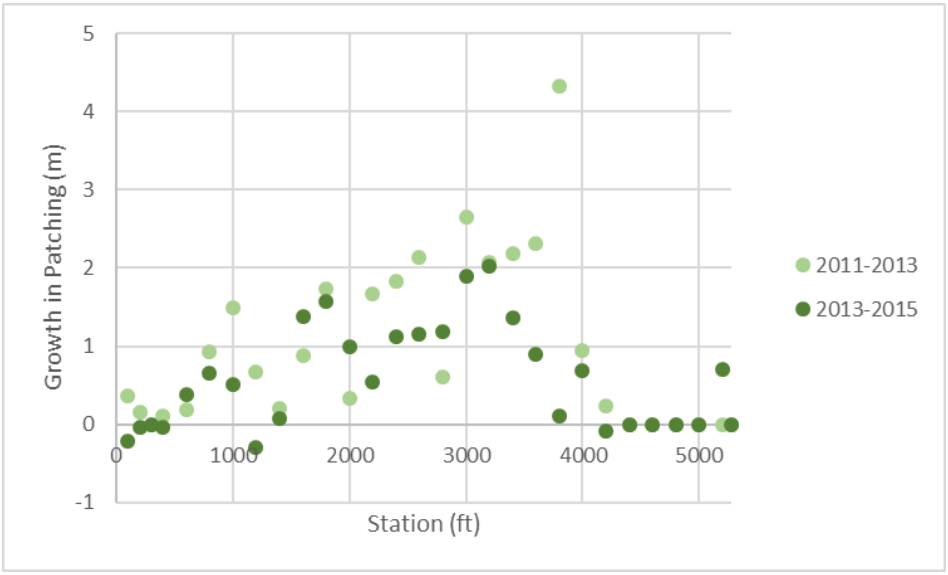

(a)

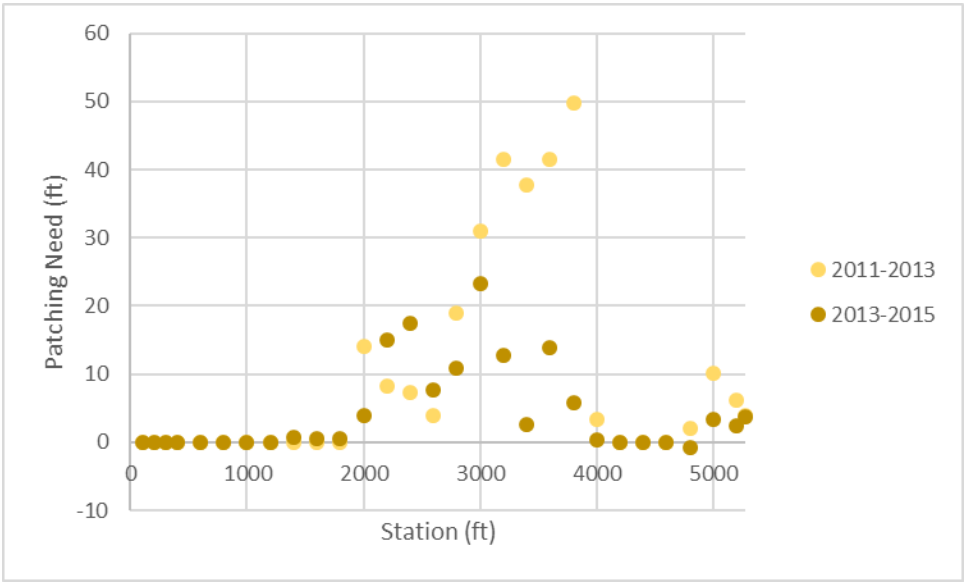

(a)

Figure 4-4 Growth in patching need for sections in (a) left and (b) right lane sides

For most cases, growth primarily happens between 2011 and 2013. However, the scale of growth varies for the left and right lane halves. For the left lane half, the growth is less than 5-m over the course of two years, and in most cases, less than 3-m. For the right lane side, however, growth is as high as 50-m within a two-year stretch. Growth of 50+ meters in a two-year span is significant because it approaches the maximum of 200-ft (~61-m) for any section. Locations with this level of growth should be identified as high-risk areas. Alternatively, although most cases indicate growth across time, in some rare cases, the proposed method detects a reduction in patching need from one time stamp to the next.

4.2.1 Evaluating the proposed method

The proposed method operates on an image-level basis and does not join multiple images together to assess the patching need within the conjoined area. Because of this, there are some occasions where the patching need in a section decreases from one time stamp to the next. For this study, five sections in the left lane side show a reduction between 2013 and 2015. Additionally, one section shows a reduction in patching need from 2013-2015 for the right lane side. After further investigation, this reduction in patching need is determined to be the result of small patches splitting across multiple images in later years. When smaller patches (<5-ft in length) are split across two images, the proposed method may not successfully identify the short need for patching in the two images as it would if the patch were contained in a single image.

The detection of these patches is important for maintaining a comprehensive full-depth patching plan; however, because of their small size, these patches are likely not a

priority to transportation engineers. In this study, these undetected patching areas show a reduction of patching extent between 0.04 and 0.7-m (0.13 and 2.3-ft) across a two-year span. In total, section in the left and right lane sides show a reduction of 0.69-m (2.3-ft) and 0.72-m (2.4-ft) respectively from this lack of detection. Although these reductions are small in comparison to overall patching need, the lack of identification does affect total patching need calculations. To better identify these areas in the future using the proposed method, images would need to be stitched together before the patching analysis is performed. However, this would require more processing power than the current proposed method. The proposed method is adequate for identifying key areas that require significant patching, however, in some rare cases, smaller patches may go undetected, possibly resulting in a small reduction in patching extent over time.

4.2.2 Isolating significant growth of patching need on US80 from 2011 to 2015

The proposed method shows good performance in identifying the patching need for a roadway across time. Using the three years of data from US80 EB MP 10 – 11, the method shows the growing need for patching through the different time stamps. In particular, the growth of patching for the middle sections is significantly higher than the sections at the beginning and end of the mile. Because the structure of the pavement and thickness of layers can change multiple times in one mile, it is difficult to compare all sections evenly. However, because the sections are 200-ft or less, adjacent sections are likely to have similar pavement structures. The short size of the sections also helps justify the assumption that adjacent sections are subject to similar traffic patterns. Given these two assumptions, the need for patching for the one mile is assessed to determine which areas show the most growth across the three time stamps.

Between the years of 2011 and 2013, stations between 30+00 and 40+00 for the right lane side experience the highest growth, typically over 30-m in the two-year time span. This suggests this area, in particular, is prone to higher amounts of damage and more accelerated deterioration. To better asses the sources of damage, the individual sections are isolated and two sections with high growth in patching need across the four years are analyzed.

4.3 Identification of Problematic Segments and Evaluation of Pavement Performance

Because of the short distance between the start and end, the individual sections are expected to have similar traffic patterns; however, because they do not deteriorate evenly, there are likely factors outside of traffic loading that affect pavement condition. This section addresses two sections with significant increase in patching need from 2011 to 2015 to determine what external factors may have caused this extreme deterioration. For this analysis, the 200-ft sections beginning at stations MP 10 +3000 and +3400 in the right lane half are analyzed. These sections are chosen because the need for patching increases 54.3-m and 55.3-m respectively from 2011 to 2015; however the intermediate section beginning at MP10 +3200 only increases 40.4-m over the same time span. This disparity indicates influence from external factors.

The section of pavement between 30+00 and 32+00 has the third highest growth across the four-year period. Beginning in 2011, the need for patching is measured as only 2.22-m (7.28-ft). Between 2011 and 2013, this need grows to 43.7-m (143.4-ft), increasing the patching need from 3.6% of the total area to 71.6% of the total area.

Between 2013 and 2015, the need for patching increases from 43.7-m to 56.5-m (185.4-ft), equal to 92.7% of the entire section requiring patching for that half of the lane. This extreme performance indicates external factors led to the accelerated damage.

This 200-ft section begins at the start of an extensive counter-clockwise horizontal turn in the highway as shown in Figure 4-5. The sections immediately before and after also contain significant need for patching indicating the roadway geometry may be the reason for the significant deterioration.

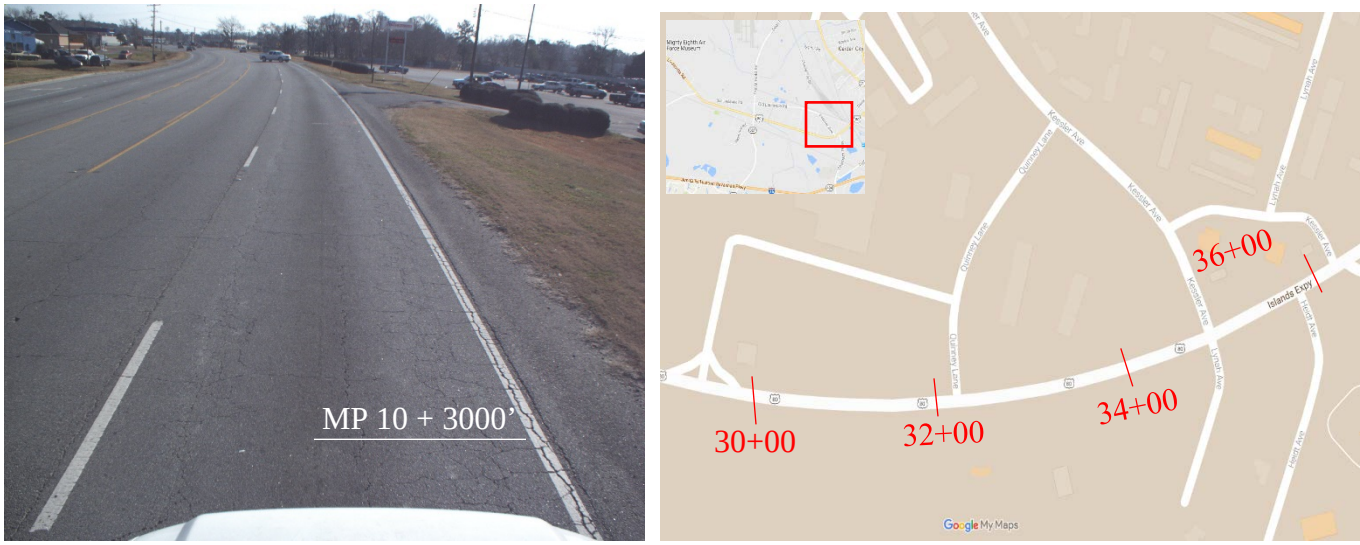

Figure 4-5 Station 30+00 to 36+00 horizontal curve

Because the section lies on a horizontal curve, as the vehicles and heavy trucks navigate this section, the weight is not distributed evenly as it would be on a tangential section. The counter-clockwise curve direction causes vehicle weight to shift to the wheels in the right wheel path, causing more damage than the left.

The damage done to the pavement is likely made worse by the heavy truck traffic through this area. There are multiple truck companies along the highway that are used to

move goods throughout the region. The heavily weighted trucks cause significantly more damage to the pavement than the passenger vehicles, and may be the separating factor in what is causing the damage to the pavement. The speed limit along this corridor may also be a factor in the damage to the pavement. The 45-mph speed limit coupled with numerous intersections results in trucks much slower than interstate highways. This slow movement means more time in contact with the pavement which causes trucks to do more damage. These factors should be considered when performing reconstruction to improve structural resilience and improve pavement life.

In comparison to the section beginning at MP10 +3000, the section beginning at MP10 +3400 is a mostly straight section with very little curve. However, the right wheel path increases significantly in patching need from 4.21-m in 2011 to 59.6-m in 2015. This significant increase is the second highest overall growth of all sections, and the reason for the significant increase likely lies in the roadway geometry. This section includes most of the approach to the major intersection of US80 and Chatham Parkway. Because of the heavy truck traffic in the area, damage at the intersection is severe due to trucks decelerating and stopping at the intersection. This causes severe rutting at the intersection which leads to ponding and water damage. Over the course of many years, the rut has continued to grow and form despite previous maintenance [29].

Using the proposed method, MP 10 – 11 are analyzed to assess the need for full-depth patching across three years. From this analysis, it is shown that the growth of patching need in the right lane side is significantly higher than that of the left lane side. By analyzing the surroundings through collected video log data, it is determined that the horizontal curvature of the road and heavy truck traffic are the likely causes of severe

damage in the right lane half. Additionally, because these sections approach an intersection, heavily-weighted trucks that drive this route are likely to slow down or sit in these sections which will accelerate the damage. Using this information, and projected traffic, better decisions can be made about how to design the pavement to withstand future accelerated damage.

4.4 Summary

The proposed method is used to evaluate multiple years of data from one mile of asphalt pavement on US80. The results from the method give the need for patching in both the left and right lane sides for 2011, 2013, and 2015. The mile is segmented into 29 sections, and the need for patching in each is measured for all three time stamps. Results primarily indicate almost all of growth of patching need is between MP10 + 2000 and MP10 +4000 with the majority occurring between MP10 +3000 and MP10 +4000. The two sections in this range with the most growth between 2011 and 2015 are examined to determine the cause for the extreme deterioration.

For most cases, growth was either zero or positive. However, for some rare cases, the proposed method failed to detect short (<5-ft in length) patch areas, resulting in a small reduction in patching need from one time stamp to the next. These failed detections account for ~2.3-ft of undetected patching area for both the left and right lane sides. Because the proposed method aims to identify the larger, more expansive patching areas, some of the shorter patching areas are not identified. On the scale of the entire mile, however, these undetected patches represent ~4% and 0.7% of the total patching need in the left and right lane sides in 2015. The current proposed method seeks to identify large

patching areas that will significantly affect cost; however, in the future, the proposed method can be improved by stitching adjacent images before performing patching need.

After assessing the patching need in all 29 sections, the results from 2011, 2013, and 2015 are compared and two sections showing significant growth are identified. The sections beginning at MP10 +3000 and MP10 + 3400 in the right lane half are identified as having significant growth from 2011 to 2015. Upon further analysis of the site and conditions, it is determined that the roadway geometry likely plays a significant role in the damage dealt to the pavement. The former section lies on a horizontal curve that is frequented by a lot of truck traffic. Because of the counter-clockwise direction of the turn, trucks navigating this turn apply more weight to the right wheel path than the left. This appears to have caused significant damage to the right wheel path over time, particularly between 2011 and 2013.

For the second site, the growth of patching need is likely a product of extended damage caused by trucks and other vehicles exiting the horizontal curve while slowing down to stop at a major intersection. The intersection of US80 with Chatham Parkway shows significant rutting damage in the wheel paths indicating severe damage from trucks sitting and waiting at the intersection. Because the test section in question includes much of the approach to the intersection, the severe increase in patching need from 2011 to 2015 is believed to be caused by damage from trucks slowing and stopping. The rutting of the pavement causes ponding of water which severely reduces the structural strength over time and accelerates the damage done by trucks. Through the proposed method, these key areas can be identified and the root of the problems can be hypothesized, leading to better decision making.

The proposed method shows promise for identifying large (>5-ft) patching areas. Using temporal data, this information can be used to identify areas that prove resilient to traffic as well as areas that require immediate attention due to their accelerated deterioration. Although the proposed method does not identify smaller patches, possibly resulting in a small decrease in patching need over time, all large patches are identified successfully. These patches often take priority over smaller patches due to their size, however for a more comprehensive full-depth patching plan, the proposed method can be altered or amended to provide a more thorough analysis if needed.

CHAPTER 5. CONCLUSIONS AND RECOMMENDATIONS

5.1 Summary of Contributions

This thesis proposes a methodology for identifying and quantifying the need for full-depth patching on flexible pavement. Chapter 2 introduces the methodology and decision making criteria for identifying these locations. Three criteria are introduced and the optimal values for identifying candidate images are determined. Using these candidate images, an image processing guide is presented to allow for crack topology analysis. To analyze crack topology, the crack polygons are identified and the centroids are clustered based on the distance between centroids and the number of centroids in the cluster. These clusters are then used to form patches. Patches are then joined with other patches based on proximity, or removed based on patch length. To further quantify need, the depth of distress is analyzed in Chapter 3.

In Chapter 3, the relationship between the surface conditions and subsurface conditions is explored using pavement cores and crack detection results. Cores are classified as intact, broken, or crumbling and the crack width and depth in the core are measured and compared to topological crack properties including crack density and weighted crack width. Through this analysis, expected crack density and average crack width values are determined for crumbling pavements that are likely to require full-depth patching. The relationships between depth of distress and surface condition is assessed; however, results are not conclusive enough to make meaningful full-depth patching quantification estimates from the collected data.

In Chapter 4, the methodology proposed in Chapter 2 is demonstrated on temporal data to assess growth of full-depth patching need. The results from this chapter show the methodology can be used for multiple timestamps to show the growth of full-depth patching need across time. Additionally, the analysis from this chapter identifies areas that have higher rates of deterioration. This allows for more thorough analysis of environmental factors that may contribute to the extreme pavement performance. The methodology shows excellent performance at identifying patching need; however there is room for improvement to facilitate better identification of smaller patching areas and depth measurement.

5.2 Directions for Future Work

The proposed methodology uses simple criteria including total crack length, average crack width, and the density of crack nodes to identify candidate images. This information is easily determined from the LCMS crack detection results, but often results in many images that do not require patching to be identified. The method could benefit significantly from using additional cracking characteristics such as the number of branch points, end points, and intersection points as criteria for identifying candidate images. This would help reduce the number of images falsely identified as requiring patching, and reduce the overall processing needed.

The processing procedure for candidate images is effective at identifying the patching need; however it requires significant processing time to identify all the crack polygons in images with severe cracking. The automated process of converting potential full-depth patching XML files to images, and processing those images to find the

polygons requires significant computing power. For this study, the XML files were converted at 1:1 scale resulting in a 5000 x 4160 px binary image. This was done to ensure all polygons in the resulting image could be successfully identified; however, in the future, by reducing the binary image size, the time required for XML conversion and polygon identification could be significantly reduced. Additionally, for this study, much of the processing time is required because the crack detection results are from the semi-automatic method. The processing time would likely be significantly reduced if an adequate, automatic crack detection method is used.

When assessing the correlation between the depth of distress and the surface condition, 13 pavement cores were used for analysis. The selected cores cover the extremes of pavement condition well. To better understand the correlation, however, more cores taken from the transitional state between structurally sound and failing need to be analyzed. These cores help better determine the variability of the data and understand the rate at which damage propagates downward through pavement layers. Additionally, although the cores used were taken from the same one mile of pavement, layer thickness and material are expected to have significant effect on the acceleration of damage. The proposed method represents a generalization from the information given, but incorporating pavement layer information is a useful step towards building a more robust model.

In addition to using pavement core samples, other, non-destructive methods can be investigated for looking at sub-surface conditions. Ground-penetrating radar (GPR) has been used to assess a multitude of properties of subsurface layers including measuring layer thickness and detect layer defects [30]. Additionally, Falling-Weight

Deflectometers (FWD) have been used as a non-destructive method of measuring the thickness and strength of pavement layers and predicting layer condition indicators [31]. The FWD can be used to measure pavement strength to determine if certain layers have begun to fail. This information can be compared to surface conditions to better understand how subsurface defects reflect to the surface.

APPENDIX A. IMAGES USED TO DEVELOP THRESHOLD CLASSIFICATION VALUES

This appendix illustrates the default style of subheadings as described in the Graduate Studies Thesis Manual, available at http://www.grad.gatech.edu/thesis. Your department may have its own style guide and its own way of formatting subheadings. Whichever scheme you use, you must use it consistently throughout the document or the Graduate Thesis Office will require you to make revisions until it is acceptable.

To estimate crack statistic threshold values for the proposed method, a set of test images were classified based on the evident need for full-depth patching (also known as 'deep patching') in the 3D pavement image. If there is an evident need for full-depth patching, the images were classified as 'deep patching (DP)' images while all other images were classified as 'no deep patching (NDP)' images. These images were then analyzed separately based on their cracking statistics. The sections below give examples of these two types of images and the need for patching in each image.

A.1 Full-Depth Patching (DP) Images

These images are classified by severe cracking in the 3D pavement image. The cracking is typically load cracking severity level 3 or 4 as measured by the GDOT PACES manual. This type of cracking has multiple longitudinal cracks (driving direction) connected by transverse (across the width of the travel lane) cracks. Examples of these images are given below and the limits of patching required are highlighted in each image.

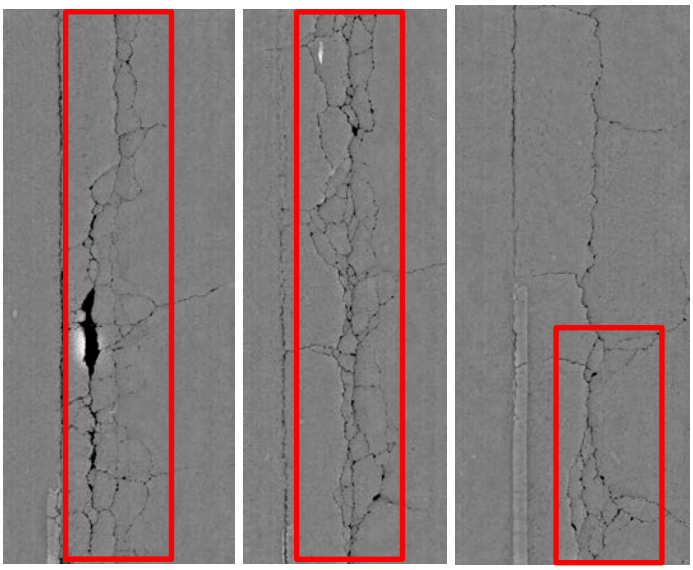

(a) (b) (c)

Figure A-1 Images requiring full-depth patching in the lane half

The need for full-depth patching is evident in these images because of the multiple longitudinal cracks connected by transverse cracks. In Figure A-1a, the need for patching extends to the top of the image although the cracking is less severe in the top half. Although the top half of the image would likely be classified as severity level 2 load cracking according to PACES, it is still included in the patching area. This is because areas like this are severely damaged and may deteriorate quickly if not patched. For Figure A-1c, the patch outlined using the proposed method close follows the severe cracking at the bottom of the image, but does not include the singular longitudinal crack above it.

A.2 Images Not Requiring Full-depth Patching.

Images that do not require full-depth patching are typically easier to identify because they generally have little to no cracking in the image. The lack of cracking

makes them stand out visually and also helps the classification process because they can be easily removed by the short total crack length (TCL) in the image. Examples of these images are given below in Figure A-2.

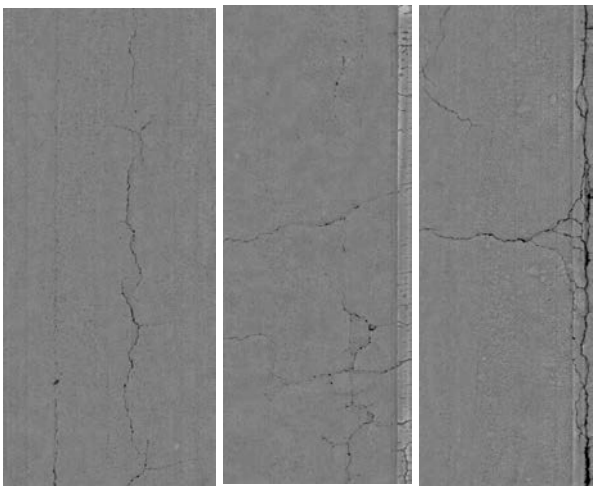

(a) (b) (c)

Figure A-2 Images not requiring full-depth patching

The above images show low levels of cracking and therefore would not require full-depth patching. The low density of cracking indicates the surface layer is mostly intact and can handle the traffic loads being applied. In Figure A-2b, there is a more severe concentration of cracking in the bottom portion of the image. Although this may represent severity level 2 or 3 load cracking, the size of the patch formed around this section would likely be too small for proper patching equipment. For Figure A-2c, the need for patching extends outside of the travel lane. For this study, only the pavement between the lane markings is used, therefore this image has no patches detected.

APPENDIX B. PAVEMENT CORE IMAGES

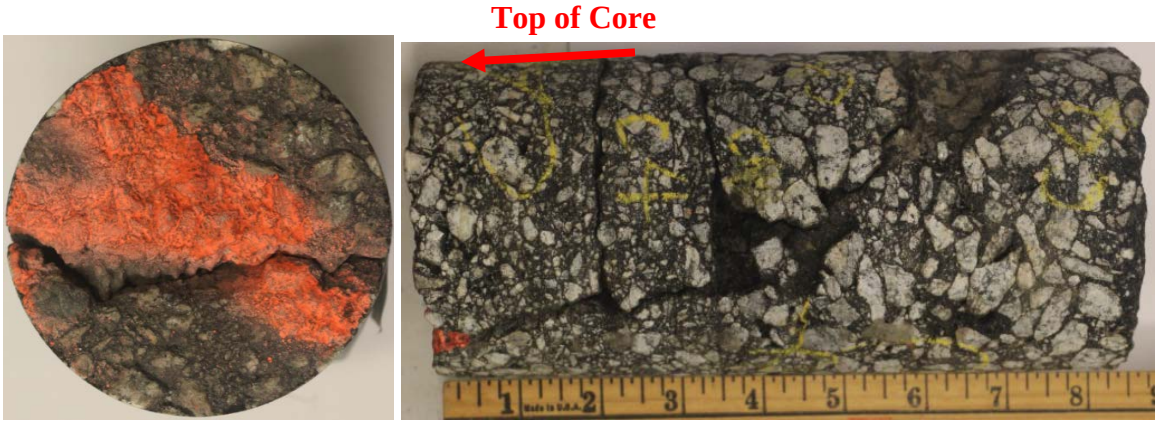

(a) **(b)**

Figure B-1 Core C4 a) top and b) side

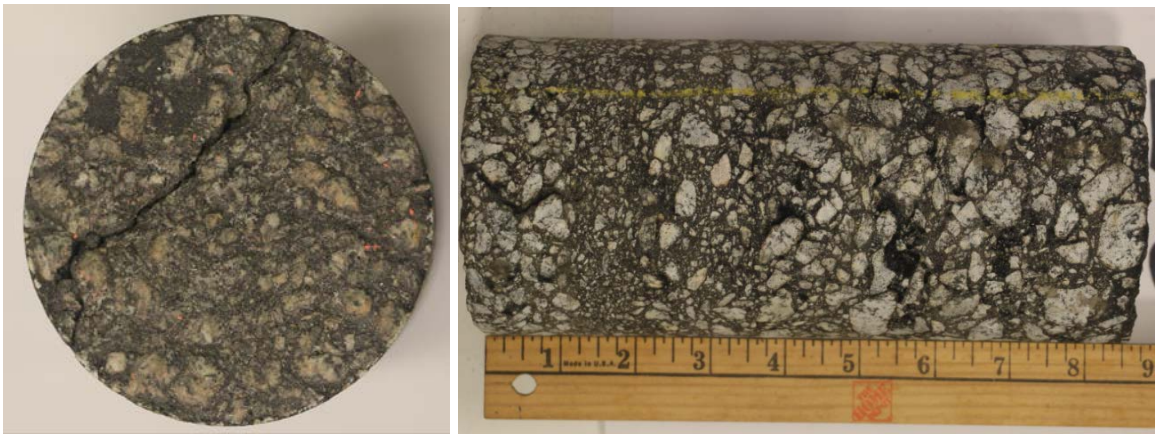

(a) **(b)**

Figure B-2 Core C5 a) top and b) side

(a) **(b)**

Figure B-3 Core C6 a) top and b) side showing bottom-up cracking

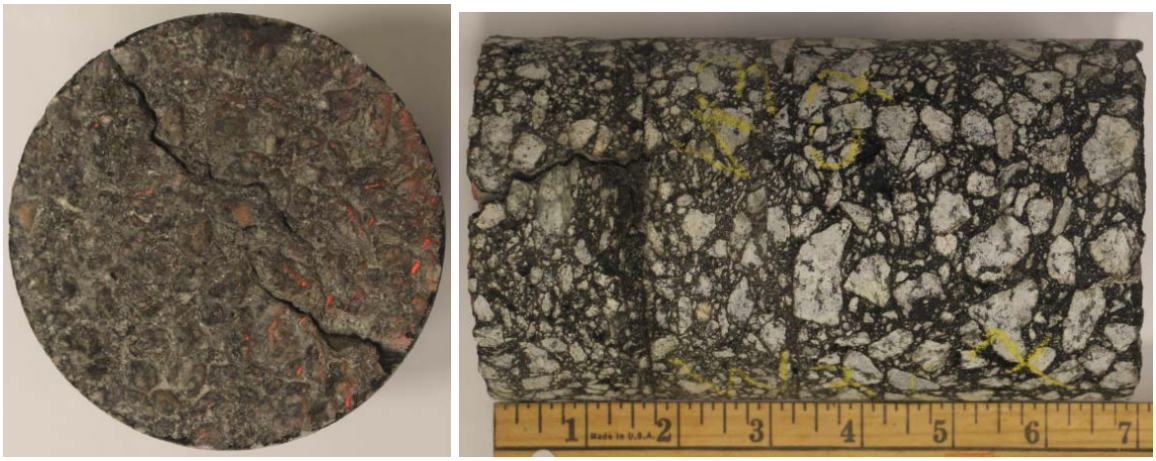

(a) **(b)**

Figure B-4 Core C7 a) top and b) side

(a) **(b)**

Figure B-5 Core C8 a) top and b) side showing bottom-up cracking

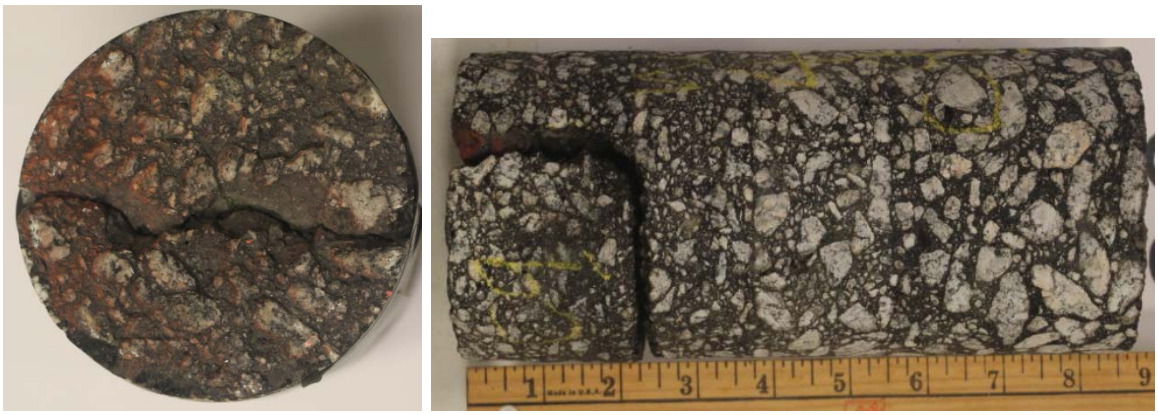

(a) **(b)**

Figure B-6 Core C9 a) top and b) side

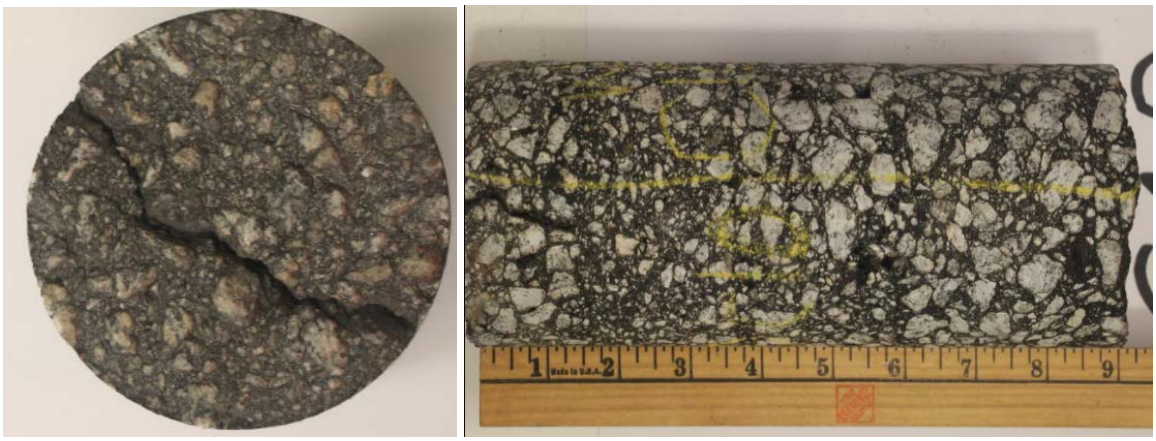

(a) **(b)**

Figure B-7 Core C10 a) top and b) side

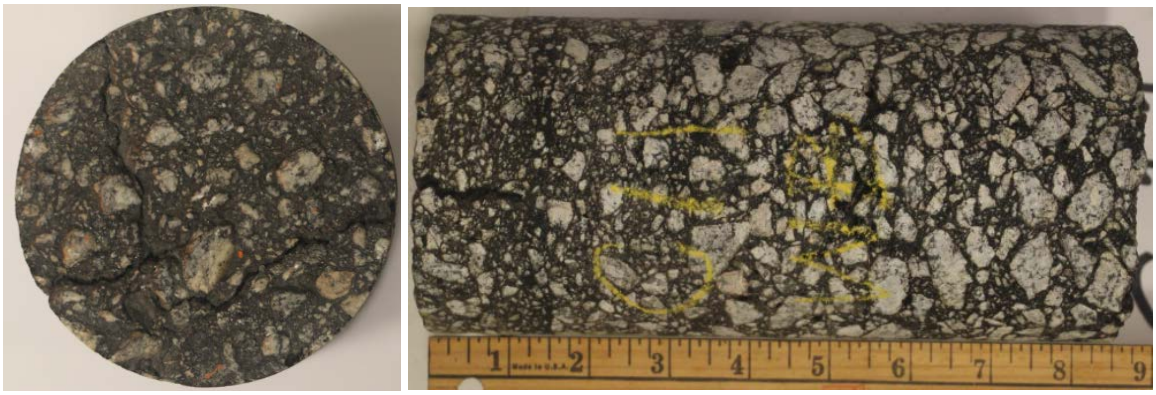

(a) **(b)**

Figure B-8 Core C11 a) top and b) side

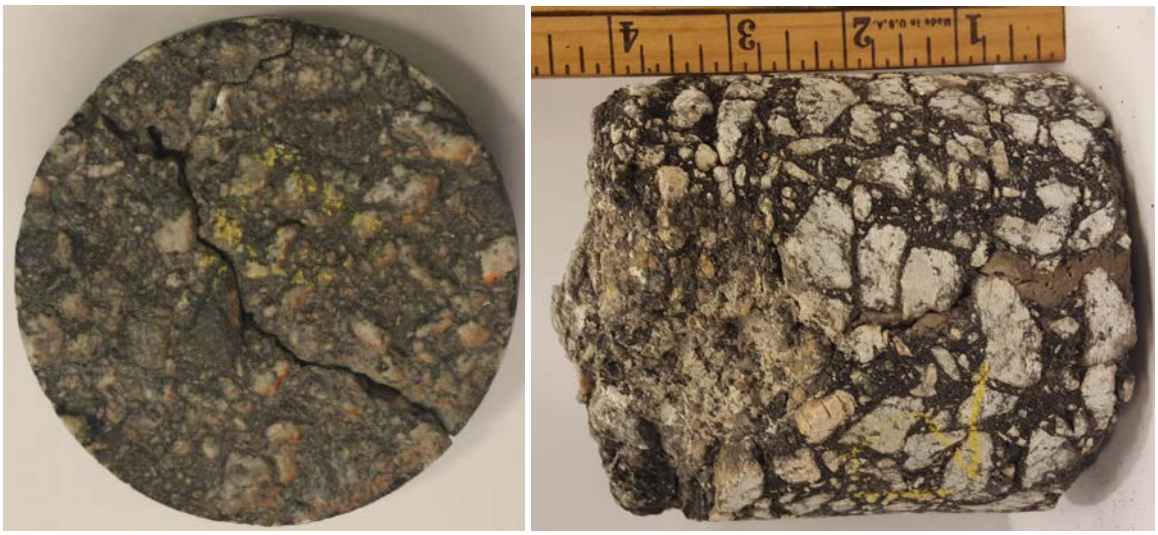

(a) **(b)**

Figure B-9 Core C12 a) top and b) side showing bottom-up cracking

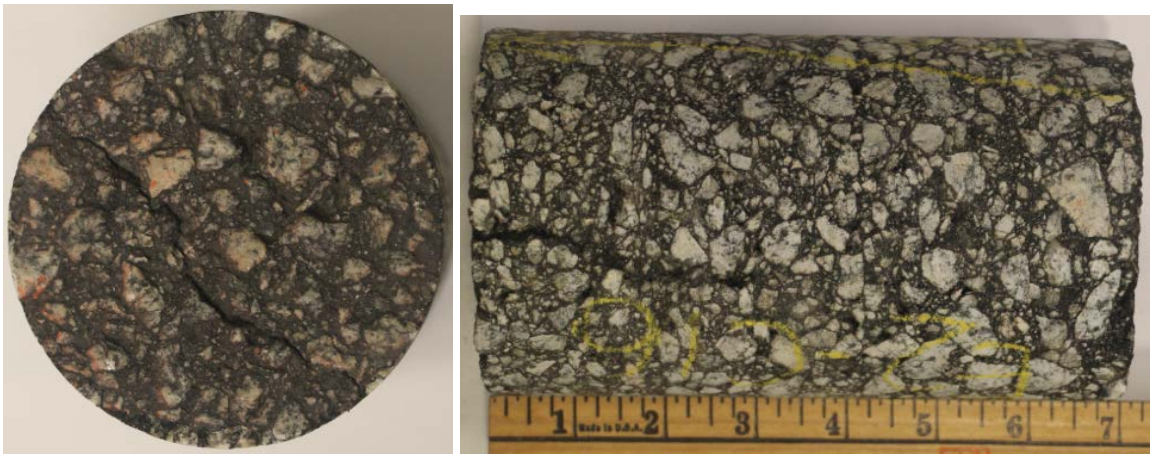

(a) **(b)**

Figure B-10 Core C16 a) top and b) side

(a) **(b)**

Figure B-11 Core C18 a) top and b) side

(a) **(b)**

Figure B-12 Core C19 a) top and b) side

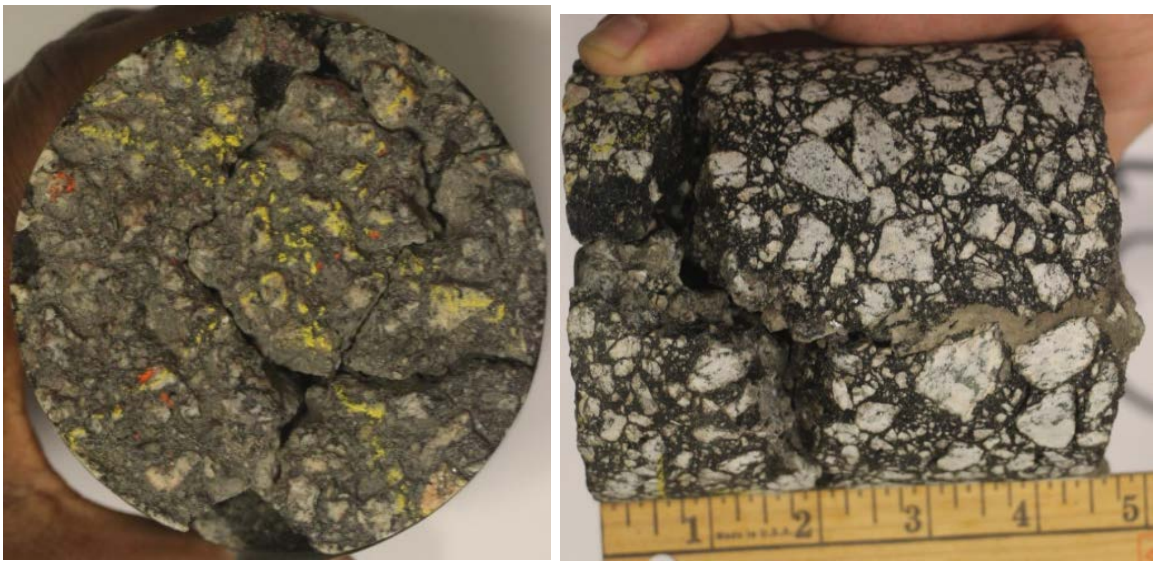

(a) **(b)**

Figure B-13 Core C21 a) top and b) side showing bottom-up cracking

APPENDIX C. PROPOSED METHODOLOGY VALIDATION WITH CRUMBLING CORES

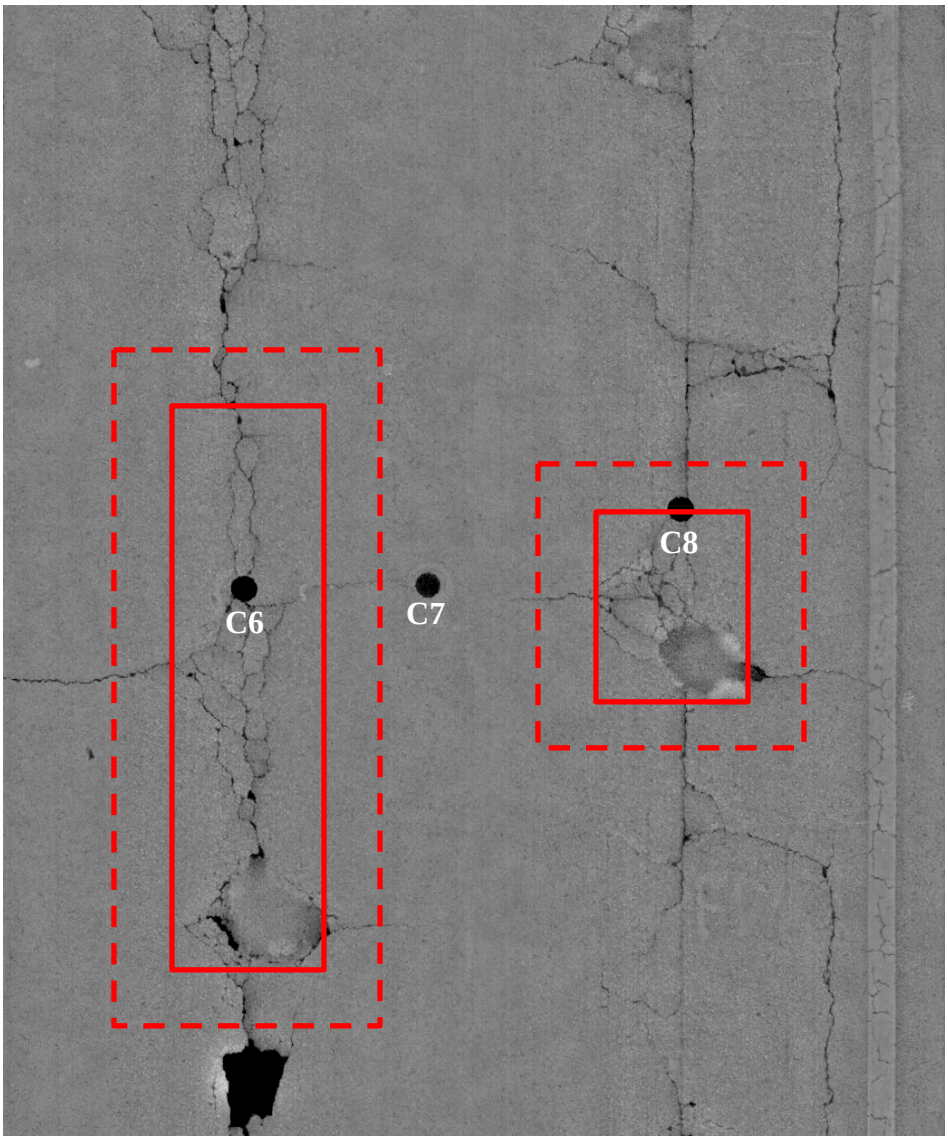

Figure C-1 Cores C6, C7, and C8 with detected patch area (solid) and 1-ft buffer (dashes)

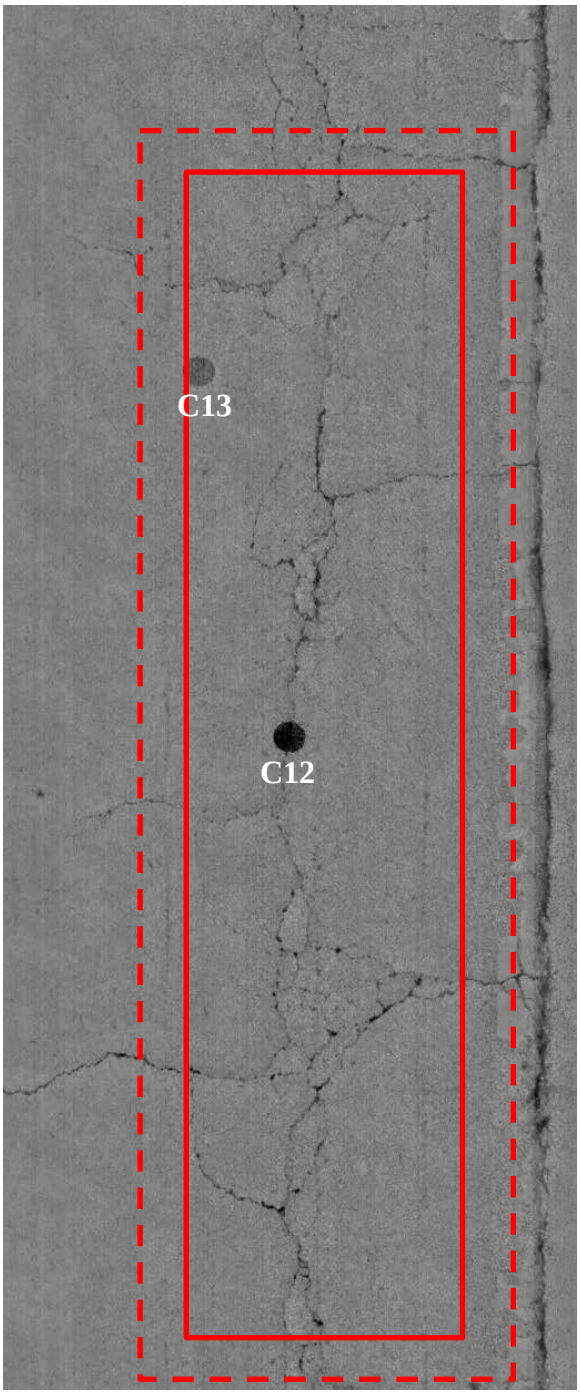

Figure C-2 Cores C12 and C13 with detected patch area (solid) and 1-ft buffer (dashes)

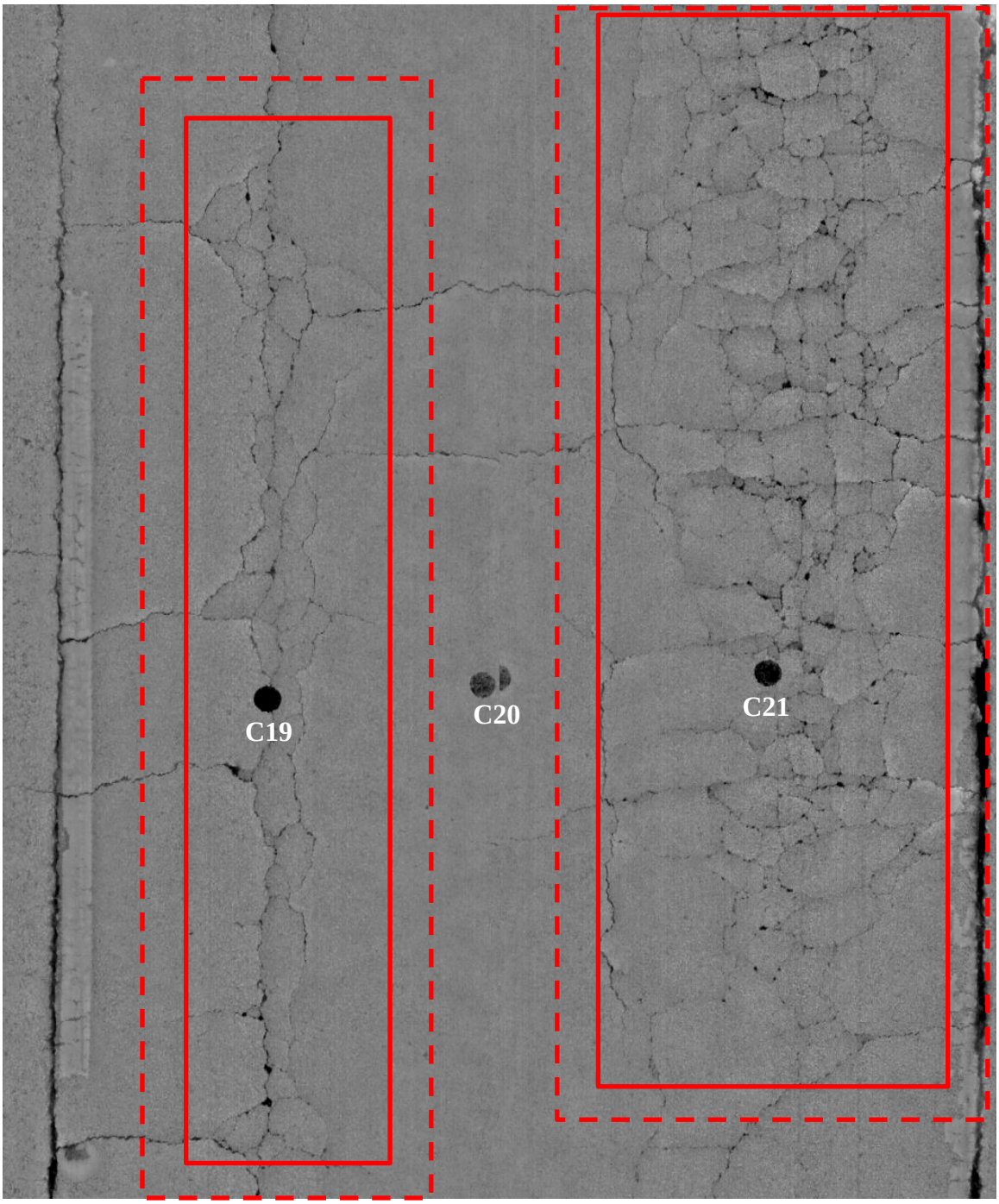

Figure C-3 Cores C19, C20 and C21 with detected patch area (solid) and 1-ft buffer (dashes)

REFERENCES

[1] American Society of Civil Engineers, "2017 Infrastructure Report Card: Roads," ASCE, January 2017. [Online]. Available: http://www.infrastructurereportcard.org/cat-item/roads/. [Accessed February 2017].

[2] Z. Wang, Y.-C. Tsai and E. Pitts, "Pavement Preservation: Pay Now or Pay Big Later," in *Compendium of Papers from the First International Conference on Pavement Preservation*, Newport Beach, 2010.

[3] G. D. o. Transportation, "PACES," Office of Maintenance, 2007.

[4] Iowa Department of Transportation, "Section 2529. Full Depth Finish Patches," in *Standard Specifications with GS-15004 Revisions*, Ames, IA, 2015.

[5] D. H. Timm and J. M. McQueuen, "A Study of Manual vs. Automated Pavement Condition Surveys," Alabama Department of Transportation, Montgomery, 2004.

[6] D. J. Findley, C. M. Cunningham and J. E. Hummer, "Comparison of mobile and manual data collection for roadway components," *Transportation Research Part C: Emerging Technologies*, vol. 19, no. 3, pp. 524-540, 2011.

[7] M. J. H. Mohajeri and P. J. Manning, "ARIA (TM): An operating system of pavement distress diagnosis by image processing," *Transportation Research*

Record, pp. 120-130, 30 April 1992.

[8] H. Rababaah, D. Vrajitoru and J. Wolfer, "Asphalt pavement crack classification: A comparioson of GA, MLP, and SOM," in *Proceedings of Genetic and Evolutionary Computation Conference*, 2005.

[9] K. M. Chua and L. Xu, "Simple procedure for identifying pavement distresses from video images," *Journal of Transportation Engineering*, vol. 120, no. 3, pp. 412-431, 1994.

[10] H. D. Lee and J. Kim, "Development of a crack type index," *Transportation Research Record*, vol. 1940, pp. 99-109, 2005.

[11] H. D. Cheng, J.-R. Chen, C. Glazier and Y. G. Hu, "Novel approach to pavement cracking detection based on fuzzy set theory," *Journal of Computing in Civil Engineering*, vol. 13, no. 4, pp. 270-280, 1999.

[12] T. Saar and O. Talvik, "Automatic asphalt pavement crack detection and classification using neural networks," in *Electronics Conference (BEC)*, Tallinn, 2010.

[13] B. J. Lee and D. H. Lee, "Position-invariant neural network for digital pavement crack analysis," *Computer-Aided Civil and Infrastructure Engineering*, vol. 19, no.

2, pp. 105-118, 2004.

[14] J. Chou, W. A. O'Neill and H. D. Cheng, "Pavement distress classification using neural networks," in *Systems, Man, and Cybernetics*, San Antonio, 1994.

[15] M. S. Kaseko, Z.-P. Lo and S. G. Ritchie, "Comparison of traditional and neural classifiers for pavement-crack detection," *Journal of Transportation Engineering*, vol. 120, no. 4, 1994.

[16] H. N. Kourtopoulos, I. El-Sanhouri and A. B. Downey, "Analysis of segmentation algorithms for pavement distress images," *Journal of Transportation ENgineering*, vol. 119, no. 6, pp. 868-888, 1993.

[17] H. N. Koutsopoulos and A. B. Downey, "Primitive-based classification of pavement cracking images," *Journal of Transportation Engineering*, vol. 119, no. 3, pp. 402-418, 1993.

[18] A. Georgopoulos, A. Loizos and A. Flouda, "Digital image processing as a tool for pavement distress evaluation," *ISPRS Journal of Photogrammetry and Remote Sensing*, vol. 50, no. 1, pp. 23-33, 1995.

[19] Y.-C. Tsai and F. Li, "Critical assessment of detecting asphalt pavement cracks under different lighting and low-intensity contrast conditions using emerging 3D

laser technology," *Journal of Transportation Engineering,* vol. 138, no. 5, pp. 649-656, 2012.

[20] Y.-C. Tsai, C. Jiang and Y. Huang, "Multiscale crack fundamental element model for real-world pavement crack classification," *Journal of Computing in Civil Engineering,* vol. 28, no. 4, 2014.

[21] Y. Huang and Y.-C. Tsai, "Crack fundamental element for multi-scale crack classification," in *7th RILEM International COnference on Cracking in Pavements,* 2012.

[22] V. Kaul, A. Yezzi and Y.-C. Tsai, "Detecting curves with unknown endpoints and arbitrary topology using minimal paths," *IEEE Transactions on Pattern Analysis and Machine Intelligence,* vol. 34, no. 10, pp. 1952-1965, 2012.

[23] C. Jiang, *A crack detection and diagnosis methodology for automated pavement condition evaluation,* Atlanta: Georgia Institute of Technology, 2015.

[24] T. Garbowski and T. Gajewski, "Semi-automatic inspection tool of pavement condition from three-dimensional profile scans," *Procedia Engineering,* vol. 172, pp. 310-318, 2017.

[25] J.-S. Chen, K.-Y. Lin and S.-Y. Young, "Effects of crack width and permeability on

moisture-induced damage of pavements," *Journal of Materials in Civil Engineering,* vol. 16, no. 3, pp. 276-282, 2004.

[26] MathWorks, "bwconncomp," 2017. [Online]. Available: https://www.mathworks.com/help/images/ref/bwconncomp.html.

[27] FHWA, "Distress Identification Manual for the Long-Term Pavement Performance Program," June 2003. [Online]. Available: https://www.fhwa.dot.gov/publications/research/infrastructure/pavements/ltpp/reports/03031/03031.pdf. [Accessed March 2017].

[28] GDOT, "Traffic Counts," Traffic Server, 2017. [Online]. Available: http://trafficserver.transmetric.com/gdot-prod/tcdb.jsp?siteid=0510265. [Accessed May 2017].

[29] C. Wang, "A Spatiotemporal Methodology for Pavement Rut Characterization and Deterioration Analysis Using Long-Term 3D Pavement Data," Atlanta, GA: School of Civ. and Env. Eng., 2017.

[30] T. Saarenketo and T. Scullion, "Road evaluation with ground penetrating radar," *Journal of Applied Geophysics,* vol. 43, no. 2, pp. 119-138, 2000.

[31] B. Xu, S. R. Ranjithan and Y. R. Kim, "New relationships between falling weight deflectometer deflections and asphalt pavement layer condition indicators," *Transportation Research Record,* vol. 1806, pp. 48-56, 2002.